UNIVERSITÀ DEGLI STUDI DI MILANO
FACOLTÀ DI SCIENZE E TECNOLOGIE

ON TWO LINEAR ASSIGNMENT PROBLEMS: RANDOM ASSIGNMENT AND EUCLIDEAN BIPARTITE MATCHING

LAUREA MAGISTRALE IN FISICA

MATTEO PIETRO D'ACHILLE

Matr. 826043

PACS: 05.10.-a

Relatore: Prof. Sergio Caracciolo
Relatore esterno: Gabriele Sicuro, Ph.D.

Università degli Studi di Milano
Facoltà di Scienze e Tecnologie
Dipartimento di Fisica
Martedì 12 aprile 2016

Anno Accademico 2014/2015

Matteo Pietro D'Achille: *On two linear assignment problems: Random Assignment and Euclidean Bipartite Matching* , Laurea Magistrale in Fisica, martedì 12 aprile 2016.

sunt igitur venti ni mirum corpora caeca
quae mare, quae terras, quae denique nubila caeli
verrunt ac subito vexantia turbine raptant,
nec ratione fluunt alia stragemque propagant
et cum mollis aquae fertur natura repente
flumine abundanti, quam largis imbribus auget
montibus ex altis magnus decursus aquai
fragmina coniciens silvarum arbustaque tota,
nec validi possunt pontes venientis aquai
vim subitam tolerare: ita magno turbidus imbri
molibus incurrit validis cum viribus amnis,
dat sonitu magno stragem volvitque sub undis
grandia saxa, ruit qua quidquid fluctibus obstat.

— Lucretius, **De Rerum Natura**, Liber I, vv.277-294

ACKNOWLEDGEMENTS

The development of this thesis work would have been impossible without the unconditional help of a number of people since times in which the probability of this day to occur was nearly zero.

I will address people by subsets of non-decreasing cardinality.

Academia I would like to express my sincerest thanks to Professor Sergio Caracciolo for his supervising work. The wideness of his vision has been for me a continue source of inspiration. I address also my sincere thanks to Gabriele Sicuro for the many intercontinental calls had during the realization of the thesis.

Parents and relatives Your support is inestimable. I thank my parents Domenico and Lucia for giving me the possibility to study. I'm harnessing this wonderful gift with all my heart.

Friends & acquaintances I am particularly grateful to F. Arrigoni, G. Di Corato, P. Benetti Genolini, M. Gigli and A. Lerose for the many interesting discussions we're still having in spite of the distances.

I thank the whole "group of skepticals" in Monza & hinterland: you're growing well and I'm pleased to have been chosen as your guide in the mare magnum of disinformation. I generally thank the many people in there for the many fruitful experiences which we've shared.

I'm thankful to all my past schoolmates for the many formative (and sometimes singular) experiences we've done together. They are well nested inside my cultural baggage.

Milano, martedì 12 aprile 2016 Matteo Pietro D'Achille

SOMMARIO

A partire dal lavoro seminale di Mézard e Parisi in Mézard e Parisi, 1985 si è assistito ad una crescente commistione tra i metodi della teoria dei sistemi disordinati a bassa temperatura ed alcuni problemi complessi di ottimizzazione combinatoria alle cui diverse configurazioni è possibile associare un costo, che in meccanica statistica prende il significato di una energia. Parte di questo interesse nasce dal fatto che, pure in presenza di disordine, da un lato le simulazioni al calcolatore hanno mostrato comportamenti ricchi per tutta una classe di modelli, e dall'altro, le tecniche della fisica hanno permesso per la prima volta di ottenere risultati analitici sulle loro soluzioni.

Tra i numerosi problemi che possono essere studiati in questo modo, nel presente lavoro è stato analizzato il problema dell'assegnazione lineare; esso può essere descritto ad esempio come la ricerca dell'attribuzione di n compiti ad n agenti che minimizza il tempo totale di esecuzione laddove sia noto il tempo t_{ij} impiegato dall'agente i per svolgere il compito j.

Lo svolgimento della tesi è articolato in due parti: dapprima è stata realizzata una implementazione nel linguaggio C++ dell'algoritmo di Jonker-Volgenant (Jonker e Volgenant, 1987) per la risoluzione del problema dell'assegnazione lineare; tale implementazione è stata poi impiegata nello studio del ground state del problema dell'assegnazione Euclidea in D dimensioni, dove i vincoli imposti dalla metrica rendono frustrato il sistema, e della sua approssimazione di campo medio quando $D \to \infty$, dove invece il costo dell'assegnazione è una variabile aleatoria.

ABSTRACT

The pioneering work by Mézard and Parisi Mézard and Parisi, 1985 proved that methods from the theory of disordered systems at low temperature can be used to solve very difficult combinatorial optimisation problems, being possible to assign an energy to their configurations and proceed with the usual apparatus of statistical mechanics. Moreover, numerical simulations showed reach behaviors that, as well as being approachable by replica calculations, opened a lot of interesting questions.

Among the variety of problems that one can study in this context this work focused on the linear sum assignment problem, which can be described for example as the assignment of n tasks to n workers in such a way that the total time of execution of the tasks is minimum, being known that worker i spends t_{ij} seconds to complete the task j.

The work was developed in two stages: first it was constructed and tested a C++ implementation of the Jonker-Volgenant algorithm that solves a general linear sum assignment problem; this code was used to study the Euclidean bipartite matching problem in D dimensions, where frustration is imposed by the geometry of the ambient space, and to see how this problem reaches its mean field approximation in the $D \to \infty$ limit (the random assignment problem), where the assignment cost is completely aleatory.

CONTENTS

LIST OF FIGURES

LIST OF TABLES

1 INTRODUCTION

Combinatorial optimisation may be defined as the set of results and techniques used to find extrema of some application taking values only on a finite (or at most countable) set S, where the usual apparatus of mathematical analysis is not available. A typical problem in combinatorial optimisation can be split in two parts: in the first one computes the cardinality of a set $|S|$, given certain constraints (combinatorial part); in the second part one investigates ordinability of elements $u \in S$ with respect to some function $\phi : S \to \mathbb{R}$ which we may call an "energy", the most common problems being the study of existence and uniqueness of extrema for ϕ (optimisation part). It is also of interest the study of the dependence of properties of such extrema upon the aforementioned constraints, which one can call the "boundary conditions".

Given the generality of the previous considerations it should not come unexpected that in physics and applied mathematics a very large class of problems, in particular the ones concerning probability theory, can be cast in this fashion.

At the simplest level consider for example a $n \times n$ chessboard and suppose to be interested in counting in how many ways it is possible to tile it with domino (i.e. rectangles 2×1) pieces. Moreover: is it possible to tile completely the chessboard in figure 1?

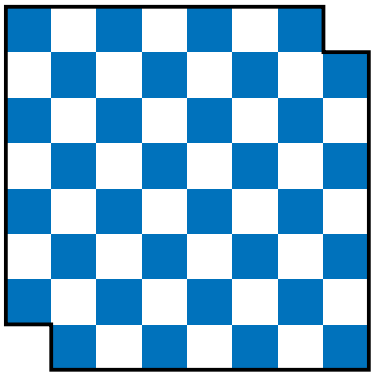

Figure 1: The 8×8 "mutilated chessboard".

The other problem mentioned in the prefaciont of Arnol'd, 2004 states: "From a barrel of wine, a spoon was poured into a cup of tea, and then the same spoon of the obtained (nonhomogeneous!) mixture was poured from the cup back into the barrel. Where did the amount of the foreign beverage become greater?"

In the preface of the first edition of Arnol'd, 2004, talking about this problem the author states literally: "Mathematical training in Moscow usually begins before the school age. Here is a couple of excercises (children 4—5 years old would have solved them in half an hour)...".

At fist glance it may seem that problems of this kind are of little or no concern to physics; but it is worth noticing that tiling problems

arise quite naturally in statistical physics, for example in the study of the macroscopic properties of a system constituted of a great number of dimer-like particles on a lattice. Maybe the most famous example of a computation involving combinatorial arguments of this kind was shown more than fifty years ago in Kasteleyn, 1961 where closed formulas for the domino-tiling problem on an arbitrary $n \times m$ chessboard are also obtained.

Computing the partition function Z of a system of course has to do with counting (or possibly measuring) all its accessible configurations (Z is the initial of the German Zustandssumme, "sum over the states"); this already difficult task becomes even harder in presence of *disorder*.

When a system is disordered (under some assumption) one can study the *average properties* of the thermodynamic quantities of interest: for example one may assume that the typical time scale of the fluctuations of the disorder can be considered infinite, a disorder of this kind being called "quenched disorder"; even showing that the relative fluctuations of extensive quantities like the free energy vanish in the thermodynamic limit is far from trivial. A thermodynamic quantity for which the previous statement holds is known in the literature as "self-averaging".

This scenario becomes even more difficult in presence of hard constraints, constraints that have little or nothing to do with disorder but are instead intrinsic to the system, reflecting geometrical or even topological features of the state space. Systems exhibiting those essential constraints are called *frustrated*. An example of topological constraint is the mutilation of the chessboard in figure 1; in this thesis work it was studied frustration of geometrical type induced by an Euclidean space.

Combinatorial optimisation is a rather broad and interdisciplinary field, its ideas stretching from theoretical computer science to statistical physics throughout graph theory, the latter providing the ground basis for both exact results and construction of efficient algorithms. One example of non trivial property that is very useful in the construction of an optimisation algorithms is that a greedy-like approach, such as the one discussed in 2.2.2 –where optimisation happens at local level during the exploration of paths on a graph– can be implemented to speed-up a certain linear program, called the linear sum assignment problem, as the paradigmatic abstract problem for all the numerical investigations of this work.

The literature implied by the previous remarks is immense; in order for this work to be as autonomous as possible, a number of choices were necessary. They can be summarized as follows.

GRAPH THEORY AND COMPUTATIONAL ASPECTS is an exposition of results in graph theory, mainly in the case of simple undirected graphs. This rather long path was taken to formulate mathematically the definition of a Linear Sum Assignment Problem, and with the aim to elucidate the primal-dual shortest-augmenting path algorithm Jonker and Volgenant, 1987 discussed in 2.3.2 that constituted the core this thesis work.

RANDOM ASSIGNMENT VS EUCLIDEAN BIPARTITE MATCHING contains the two models studied in the thesis work. They can be both formulated as linear sum assignment problems, but while in the first case correlations are induced only by the matching constraint, in the second also euclidean geometry plays a role. The relationship between those two problems is extensively investigated numerically in 3.5, with a simulation lasted two weeks of total computational time. The work done and the corresponding numerical findings are presented intertwined with already known results, recalling the literature throughout the exposition.

THE APPENDIX A contains proofs of some theorem at the heart of the algorithm, and a brief comment on a particular stochastic process that emerges in the study of the one dimensional Euclidean matching problem.

2 GRAPH THEORY AND COMPUTATIONAL ASPECTS

Contents

2.1 METHODOLOGICAL REMARK

The birth of graph theory dates back to the work of Euler, who in Euler, 1741 solved the famous puzzle about the traversability of the seven bridges of the prussian city of Koenigsberg, excluding the possibility to travel the city with a path that never returns to the same bridge. But it wasn't until the 1940's that graph theory acquired full centrality as a branch of mathematics, on top of the first monographs, in particular, as quoted in Tutte, 1984, with the publication of "the first book on graph theory" König, 1936.

See Alexanderson, 2006 for an historical point of view on Euler's pioneering works in topology during the period 1735-1759.

With its rather general setting and broad spectrum of applications, graph theory is a very fast growing area of mathematics with deep and tangled bonds in both computer science and statistical physics.

Without presumption of completeness, this section aims at fixing notations, explaining why a general linear assignment problem attains its extrema on permutation matrices, meanwhile exposing results in graph theory to elucidate the algorithm used in the thesis work, in an as personal as possible manner and with simple examples.

The textbooks consulted for the background study of this part are Chartrand and Zhang, 2012 for the foundational aspects, Tutte, 1984 for rigorous results and Steen, 2010 for the point of view of computer science and a very neat presentation of the algorithm of section 2.2.2.

2.2 GRAPH THEORY

2.2.1 Basic definitions

A **graph** G is a couple $(V(G), E(G))$ where the set $V(G)$ is the vertex set, whose elements $u, v, \ldots$ are called *vertices* or *nodes* (or *sites*), and the set $E(G)$, such that $E(G) \subset \mathcal{P}(V(G))$, is called the edge set, an element of which is called an *edge* (and sometimes a *link*, a *bond* or a *line*, depending on the contest).

Sometimes the cardinality $|V(G)|$ of the vertex set $V(G)$ of a graph G is called the *order* of the graph, and correspondingly the size of its edge set $|E(G)|$ is called the *size* of the graph; throughout this work an element of $E(G)$ is uniquely identified by a couple of vertices (say u and v): when ordering is inessential, the graph is called *undirected*; when the edge $e = (u, v) \neq (v, u)$, the graph is called *directed*, or *digraph*, and each edge can be thought to possess a *head* and a *tail*.

It is customary to refer to the structure of a graph as a collection of incidence relations, meaning that every edge is incident to exactly two vertices, while a vertex can be incident to an arbitrary number of edges. The number of edges that are incident with a certain vertex v in an undirected graph is called the *degree* or the *coordination number* of v, usually denoted as $\deg(v)$ or $\delta(v)$; the set of vertices at the other ends of the edges incoming in v, whose number adds up to $\delta(v)$, is called the *neighborhood* of v, $N(v)$.

When dealing with a digraph it is convenient to introduce the *in(out)*-degree of a vertex, indicated as in(out)deg(v), the total number of edges entering (exiting) the vertex v, and in the same spirit one defines the in(out)-neighborhood $N_{in(out)}(v)$. Clearly

$$N_{in}(v) \cap N_{out}(v) = \emptyset$$

so that $N(v) = N_{in}(v) \cup N_{out}(v)$.

A graph G is *bipartite* if two subsets exist U and V, called the *partite* sets) of the vertex set $V(G)$, in such a way that $V(G) = U \cup V$, with $U \cap V = \emptyset$ and every vertex of a partite set has its neighborhood only in the other one, i.e. $\forall u \in U\, N(u) \subset V$. A bipartite graph G with partite sets U and V is usually denoted as $G_{U,V}$

Since every edge in a graph sticks to two vertices (or to one vertex twice), the sum of the coordination numbers over all vertices of an undirected graph is always even and equals $2|E|$; in the present notation this property (known in the literature as the "handshaking lemma" since it states that the number of handshakes in an arbitrary party is always even) is

$$\sum_{v_i \in V(G)} \delta(v_i) = 2|E(G)|$$

With a slight modification this same result holds also in the theory of directed graphs.

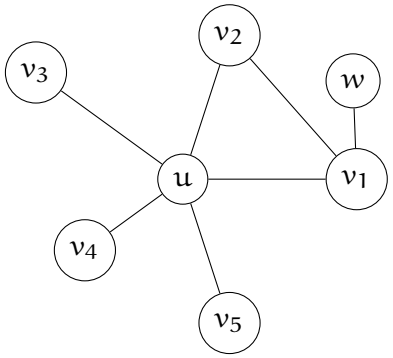

(a) A simple graph with $|V| = 7$ and $|E| = 7$

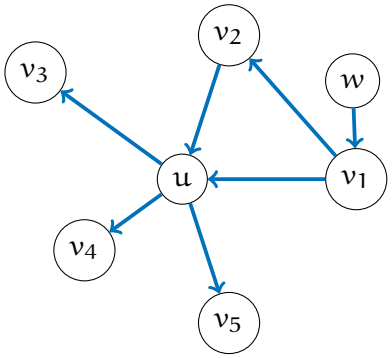

(b) One of the 128 possible orientations of the graph in figure 2a

Figure 2: In figure 2a a simple connected graph; in figure 2b a directed graph.

In a digraph an edge has exactly one head and one tail, so that

$$\sum_{v_i \in V(G)} \text{outdeg}(v_i) = \sum_{v_i \in V(G)} \text{indeg}(v_i) = |E(G)|$$

A subgraph $H \subseteq G$ is obtained by selecting a subset of $E(G)$ or $V(G)$ without violating incidence relations (i.e. $u \in V(H) \Rightarrow u \in V(G)$, $e \in E(H) \Rightarrow e \in E(G)$ and the endpoints of e are legit vertices of G).

In the first case, H is called an edge-induced subgraph, while in the second H a vertex-induced subgraph. Trivial subgraphs are the whole graph G and the graph $\emptyset$ where $V(\emptyset) \equiv V(G)$ and $E(\emptyset) = \emptyset$. Moreover if $V(H) \equiv V(G)$, H is called a *spanning subgraph* of G.

A *walk* of length l in a graph G is a list of consecutive adjacent vertices, i.e. a subset of $E(G)$ of the form

$$\{e_i\}_{i=1}^{l}, \qquad e_i \cap e_{i+1} \neq \emptyset$$

(in a digraph, this intersection must be at least the tail of e_i and the head of e_{i+1}.).

A walk is obtained starting from a vertex u and shifting to one of its neighbors, and so on, until a vertex v is reached; for this reason a walk of this type is also denoted as a u-v walk.

When in the sequence of edges constituting a walk there is no repetition, i.e. $e_i \neq e_j$, $i, j = 1, \dots l$, the walk is called a *trail*. When in the ordered list of edges composing a trail a vertex isn't repeated more than twice (except possibly the starting and ending point) the trail is called a *path* and, again, is usually prefixed by its terminations (i.e. a (u,v)-path means a path joining vertex u with vertex v). Any nontrivial path starting and finishing at the same vertex is called a *cycle*.

A G is called *connected* if $\forall v, w \in V(G)$ there exists a v-w walk. It is clear that in general multiple paths may exist between any two vertices of a graph; a union of two such paths, obtained by a concatenation of edges constitutes a cycle. This is done pictorially by "gluing" their starting end ending vertices.

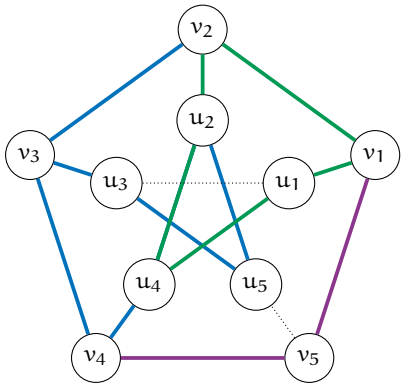

Figure 3: A walk (blue), a path (fuchsia) and a cycle (green) on a graph (see example 3 for the definition of the particular graph at hand).

The incidence relations of a graph G are usually summarized in the *adjacency matrix* $\mathrm{Ad}(G)$.

Having enumerated the vertices from 1 to $|V(G)|$, $\mathrm{Ad}(G)$ is a $|V(G)| \times |V(G)|$ matrix whose ij-th entry is the number of edges linking vertex i to vertex j, symmetrical in the case of a simple graph. This construction can be trivially extendend to digraphs; for example since the ij-th element of the adjacency matrix of a digraph D is the number of vertices exiting from vertex v_i and entering vertex v_j, one has

$$\sum_{j=1}^{|V(D)|} \mathrm{Ad}_{ij}(D) = |N_{out}(v_i)|$$

Similarly, in some case it is more advisable to work with the *laplacian* of the graph, simply defined as

$$L_{ij} = \deg(v_i)\delta_{ij} - \mathrm{Ad}_{ij} \tag{1}$$

In applications it is also useful to consider the *weighted adjacency matrix* -and correspondingly the *weighted laplacian of the graph*- that is, the matrix whose ij-th entry is some function of the edge connecting vertex i to vertex j called the *weight*. In this thesis work for example, two weighted adjacency matrices used are: one in which the i-j entry is the P-th power of the Euclidean distance between point i and point j, both chosen at random on the D-torus; and another in which the i-j entry is distributed according to a known probability density.

Another example comes from the theory of electrical networks; there the ij-th entry of the adjacency matrix is the capacity (or some other physical property of the connections). For example it is possible to state Kirchhoff laws on an arbitrary graph, as shown in Tutte, 1984, chap VI, sec.5.

Using the (weighted) adjacency matrix also unlocks tools from linear algebra, maybe the most immediate of which is finite dimensional spectral theory. This framework can be very useful to solve combinatorial problems on graphs, as the following lemma shows.

Lemma 1. *The number of triangles in an undirected graph* G *is* $\frac{1}{6}\operatorname{Tr} Ad(G)^3$.

Proof. Matrix multiplication shows that the ij-th entry of the l-th power of the adjacency matrix is

$$Ad(G)^l_{ij} = \sum_{k_1,\dots,k_l=1}^{|V(G)|} Ad_{ik_1} Ad_{k_1k_2} \cdots Ad_{k_lj}$$

So an element of this sum is a v_i-v_j walk. Since a closed walk of length 3 is necessarily cycle called also a triangle, the statement follows by taking $l = 3$ and summing on $i = j$ and recalling that we are over-counting by a coefficient $6 = 3 \times 2$, the number of entry points in a triangle times its two possible orientations. □

Example 1 (The complete graph K_n)**.** Consider the set $V(G) = \{1, \dots, n\}$ and link every vertex with the other $n-1$: the graph obtained in this way is called the complete graph and is usually referred to as K_n.

From its very definition it is clear that its adjacency matrix is

$$Ad(K_n) = \begin{bmatrix} 0 & 1 & 1 & \dots \\ 1 & 0 & 1 & \dots \\ 1 & 1 & 0 & \dots \\ \vdots & \vdots & \vdots & \ddots \end{bmatrix} \tag{2}$$

and so

$$|E(K_n)| = \sum_{i<j}^{n} Ad(K_n)_{ij} = \binom{n}{2} \tag{3}$$

the $(n-1)$-th triangular number (and the number of ways of choosing distinct couples in a set of n objects).

The characteristic polynomial of $Ad(K_n)$, which sometimes is called by extension the characteristic polynomial of K_n, can be found by simple arguments[1]. It is

$$P_n(\lambda) = (-)^n(\lambda+1)^{n-1}(\lambda+1-n) \tag{4}$$

so that, by lemma 1 and simple properties of the trace, the number of triangles in K_n equals

$$\frac{1}{6}\sum_{i=1}^{n} \lambda_i^3 = \frac{1}{6}\left[(n-1)^3 + (n-1)(-1)^3\right] = \binom{n}{3} \tag{5}$$

the $(n-2)$-th tetrahedral number and, of course, the number of distinct triples in a set of n objects, since a choice of three vertices uniquely defines a triangle.

1 As explained in the first appendix

A subgraph $H \subseteq G$ is obtained by selecting a subset of $E(G)$ without violating incidence relations (i.e. $u \in V(H) \to u \in V(G)$, $e \in E(H) \to e \in E(G)$ and the endpoints of e are legit vertices of G). Special cases of subgraphs are the whole graph G and the graph $\emptyset$.

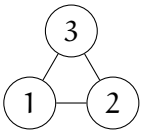

Figure 4: The complete graph K_3 is also called 3-cycle.

If $V(H) \equiv V(G)$ H is called a **spanning** subgraph of G.

The enumeration of all the spanning subgraph of a given graph G is a very interesting problem which, as already outlined in the introduction, is of key importance in the applications, as the following example shows.

Definition 1 (of trees and forests)**.** A connected graph without cycles is called a *tree*. A disjoint union of trees, i.e., a general acyclic graph is called a *forest*.

Sometimes it is useful to identify a particular vertex v of a tree, calling v the *root*; a tree with a root v is called a tree rooted at v.

Trees are the minimally connected graphs that is possible to construct, i.e., they have the least possible of edges to ensure connectivity. They are ubiquitous in pure and applied science and are completely characterized by simple properties of connectivity. One of these crucial properties is

$$|V(F)| = |E(F)| + k(F) \tag{6}$$

where $k(F)$ is the number of connected component of the forest F.

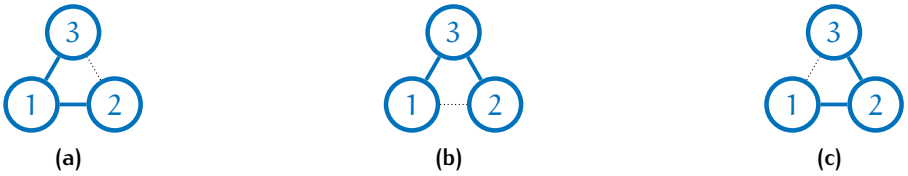

Figure 5: The 3 spanning trees of K_3.

Theorem 1 (Matrix-tree or Kirchhoff theorem)**.** *The number of spanning trees* $t(G)$ *in a graph* G *with* n *vertices is a principal minor of its laplacian matrix* $L(G)$*, i.e. the determinant of the laplacian with a row and and a column deleted and is such that*

$$t(G) = \frac{1}{n}\prod_{i=1}^{n-1}\lambda_i$$

$\{\lambda_i\}_{i=1}^{n-1}$ *being the eigenvalues of* $L(G)$ *relative to its Rank.*

A proof of this theorem that uses only a simple counting argument can be found in Godsil and Royle, 2001 (stated as theorem 13.2.1).

Example 2 (The number of spanning trees on the complete graph K_n)**.** The spectrum of $L(K_n)$ can be inferred by noticing that the adjacency matrix $Ad(K_n)$, whose spectrum is given by 4, commutes with the diagonal degree matrix.

The eigenvalues of $L(K_n)$ are obtained simply shifting all the eigenvalues of $Ad(K_n)$ by $n-1$, i.e.

$$P_n(\lambda)^{lap} = P_n(\lambda + n - 1)^{adj} = (-)^n\lambda(\lambda - n)^{n-1} \tag{7}$$

theorem 1 implies that the number of spanning trees of the complete graph K_n is n^{n-2}, the well known Cayley formula that also counts the number of distinct labelled trees with n nodes.

2.2.2 Dijkstra's Algorithm

Consider the following problem: we are given n cities and the possible roads connecting them together with all the relative distances. In general, as usual in real world scenario, a graph representing this network of roads allows cycles, whereas multiple routes are possible between each couple of cities (i.e. the underlying graph is not a tree). Starting from a certain city, what is the shortest path connecting two of them?

This problem has great relevance for example in communication networks, swapping roads with web connections and cities with servers. There one is interested in finding the shortest route according to some cost function, such as the elapsed time or the band occupied to establish a connection.

A rather elegant greedy-like algorithm to solve this problem is based on the observation that subsets of a shortest path are necessarily the shortest paths between their endpoints: a shortest path between three or more vertices can always be thought incrementally.

This local property is at the core of the most used algorithm used in the construction of the *shortest-path tree* or *geodesic tree* of a connected graph, firstly proposed in Dijkstra, 1956

The procedure at hand is discussed in Problem 2 of Dijkstra's paper. In fact Problem 1 is more of a global type, dealing with the search of a minimum spanning tree, that is, the tree T for which $\sum_{e\in E(T)} w(e)$ is minimum. Such a tree is generally different from a shortest path tree. Another somehow greedy solution of the minimum weight spanning tree problem can be found in Kruskal, 1956.

An implementation of this algorithm in fact outputs not only a single shortest path, but the entire *shortest-path-tree* rooted at some vertex s called the *sink*, that is, *all* the shortest paths emanating from the sink.

To elucidate consider a simple weighted graph G with sink $s \in V(G)$ and $|V(G)| = n$. The development of this algorithm may be described as follows.

1. Assign "intensities" to vertices: the value 0 to s, and ∞ to the other n-1.
2. Construct the set $B(s)$ of the already browsed vertices, that contains nodes towards which the shortest path starting at s has already been computed. Clearly at the first execution $B(s) = s$.
3. Consider the reachable set $R(s) = \cup_{v\in B(s)} N(v) \setminus B(s)$. Given $u \in R(s)$, a closest element to $B(s)$, update its intensity as $I(u) \leftarrow w(u)$, $w(B(s), u)$ being the shortest weight of an edge connecting u to $B(s)$. Add u to $B(s)$.
4. Iterate step 3 until $B(s) = V(G)$.

This approach can be applied to both undirected and directed graph with minor modifications.

Example 3 (Geodesics on the Petersen graph)**.** A *geodesic* between two vertices u,v in a graph G is a synonym for a shortest (u,v)-path.

The Petersen graph P is a cubic graph (i.e. $\forall v_i \in P\ \delta(v_i) = 3$) with ten vertices and many interesting properties that make it the perfect playground for counterexample in graph theory (see for example Chartrand and Zhang, 2012, sec.8.5 for an historical perspective).

Here we want to find the shortest-path tree rooted at a certain arbitrary vertex that we have chosen as the sink (the biggest blue vertex in figures 6a - 6f) by means of the Dijkstra's algorithm.

During the necessary stages to algorithm to terminate – on account of the limited space available only six of the ten stages are depicted – the set $B(s)$ is colored in blue, the reachable set $R(s)$ in green; edge weight's labels and intensities are omitted again for clarity and is established the convention that the edge pointing to the next vertex to be added to $B(s)$ is the only thick line connecting a vertex of $B(s)$ to one of $R(s)$.

At the end all nine shortest path from the sink to the other vertices are available.

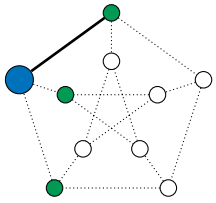

(a) At initialization, the sink is the big blue vertex. Its neighborhood is colored in green.

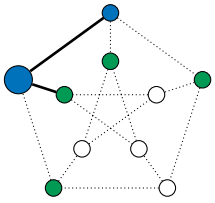

(b) At the first iteration, the set of browsed vertices $B(s)$ grows by one.

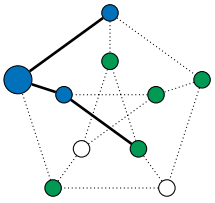

(c) At the third stage the reachable set (depicted in green) is almost the entire vertex set.

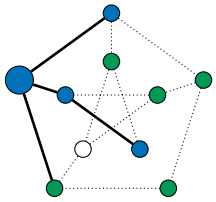

(d) During the fourth stage only one vertex is unreachable.

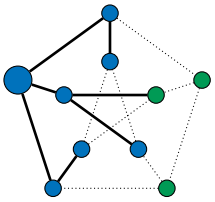

(e) At the seventh stage the reachable set is the entire vertex set.

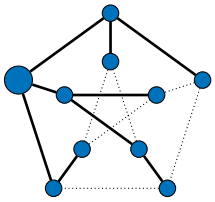

(f) After ten stages the construction of the shortest-path tree is completed .

Figure 6: Dijkstra's algorithm execution on the Petersen graph.

2.2.3 Matching theory

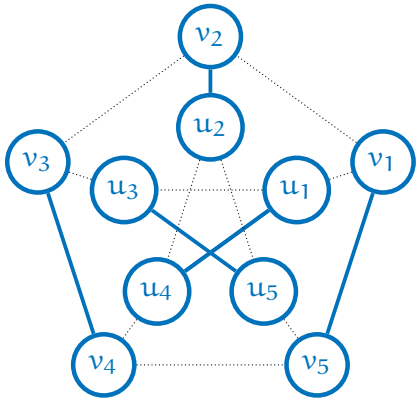

Figure 7: A perfect matching on the Petersen graph.

Consider a connected graph G. A *matching* M is a subset of $E(G)$ having the property that no two of its edges are adjacent; equivalently M is a collection of edges in which a vertex is found at most one time.

A matching M is called perfect for a graph G if every vertex of G figures in one (and exactly one) of the edges of M.

The (spanning) subgraph induced by a perfect matching is also called a *1-factor*, since $\delta(v_i) = 1, \forall i = 1, \dots, n$; in general one can define the *k-factor* of a graph as the maximum spanning k-regular subgraph; clearly if a graph G has a 1-factor then $|V(G)|$ is an even number.

This work focused on bipartite perfect matching, since this framework catches the fact that vertices stay in two different classes that have to be coupled, such as the black and white points of section 3.3, ladies and gentlemen that have to be married, requests of web pages from n browsers to m servers, workers and tasks that have to be assigned to them, and so on.

Perfect matchings in the complete bipartite graph $K_{n,n}$, also called *assignments*, are the central objects of paragraph 2.3.1.

A characterizing –and somehow surprising, at least in its sufficient part– result on matchings for bipartite graphs is the following.

Theorem 2 (Hall). *A necessary and sufficient condition for a bipartite graph* $G_{A,B}$ *(say without loss of generality* $s = |A| \leqslant |B|$*) to have a matching of cardinality* s *is* $|H| \leqslant |N(H)|$*, for all* $H \subset A$.

A constructive proof is given in A.1.2. The condition in theorem 2 (known in the literature as Hall's condition) states that every subset of vertices, as a whole, must have an appropriate number of neighbors. Note that this theorem closes on a rigorous basis the truncated chessboard problem mentioned in the introduction, where the partite sets of blue squares B and white squares W violate Hall's condition

$$30 = |W| = |N(B)| < |B| = 32$$

It is clear that, by the very definition, the number of perfect matchings in a simple graph G is the permanent of its adjacency matrix:

$$\operatorname{perm}(Ad(G)) = \sum_{\sigma \in S_n} \prod_{i=1}^{n} Ad_{i\sigma(i)}$$

2.3 LINEAR ASSIGNMENT PROBLEMS

2.3.1 General considerations

A *linear assignment problem*, called sometimes a "linear sum assignment problem", is the search of an assignment of n objects of one kind (say the jobs) to n objects of another kind (say the workers) given a certain cost per work c_{ij} in such a way that the *objective function* or *total cost*

$$O(\pi) = \sum_{i=1}^{n} c_{i\pi(i)} \tag{8}$$

attains its minimum. In this way an assignment on a bipartite graph is a synonym for an invertible map from a finite set into itself, a *permutation*, so that in full generality the search has to be conducted between all the $n!$ elements of the symmetric group S_n. It is clear that a brute force approach would rapidly become unpractical.

It is convenient to restate the assignment problem in a slightly different way writing down explicitly the constraints of injectivity and surjectivity of the assignment.

$$\begin{aligned} &\text{find } \min \sum_{i,j=1}^{n} c_{ij} x_{ij} \\ \text{under constraints} \quad &\sum_{a=1}^{n} x_{ab} = 1 \qquad b = 1, \dots, n \\ &\sum_{b=1}^{n} x_{ab} = 1 \qquad a = 1, \dots, n \\ &x_{ab} \in \{0, 1\} \qquad a, b = 1, \dots, n \end{aligned} \tag{9}$$

A matrix x_{ab} respecting the three constraints in (9) is called a permutation matrix.

If only the third constraint is relaxed to $x_{ab} \in \mathbb{R}^+,\ a, b = 1, \dots, n$, matrix x_{ab} is called *doubly stochastic*. Matrices of this type arise for example in the theory of Markov chains, where the i-j entry is the probability of transition from state i to state j.

A very important result characterize uniquely doubly stochastic matrices.

Theorem 3 (Birkhoff-Von Neumann)**.** *Every doubly stochastic matrix is a convex combination of permutation matrices.*

A proof is in the appendix A. In this way we are thinking at the set of doubly stochastic matrices of fixed size, called the *assignment politope*, as immersed in an ambient space. One can show that it is the smallest convex set containing all of its vertices (the $n!$ permutation matrices). A closed set of this type is called a *convex hull* of its vertices. One can think at $n \times n$ permutation matrices as points in $\mathbb{R}^{n^2}$ and study the properties of this polytope. The importance of theorem 3 stems from the fact that optimal solutions (for an objective function of the type at hand) have to be attained at the vertices of the assignment polytope which are the permutation matrices representing perfect matchings. It is now possible to implement a strategy to solve the linear assignment problem with relaxed constraints, the solution being "automatically" a permutation matrix (in fact one can prove the logical equivalence of Hall's and Birkhoff-Von Neumann theorems).

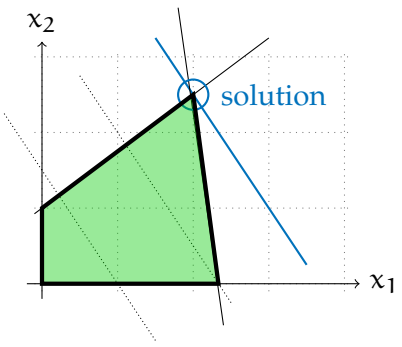

Figure 8: An objective function of type such as (8) attains its extrema on the vertices of a polytope.

To see how this strategy works, from now on the setting will be exclusively that of a certain bipartite graph $G_{U,V}$, where $U = \{u_i\}_{i=1}^{|U|}$ and $V = \{v_i\}_{i=1}^{|V|}$. Consider a known matching M: we want to construct a procedure that increases its cardinality and that assures optimality. To this end, consider an alternating path, a path for the matching M that is constituted of edges alternatively in M and not in M such as the one connecting u_1 to v_4 in figure 9a.

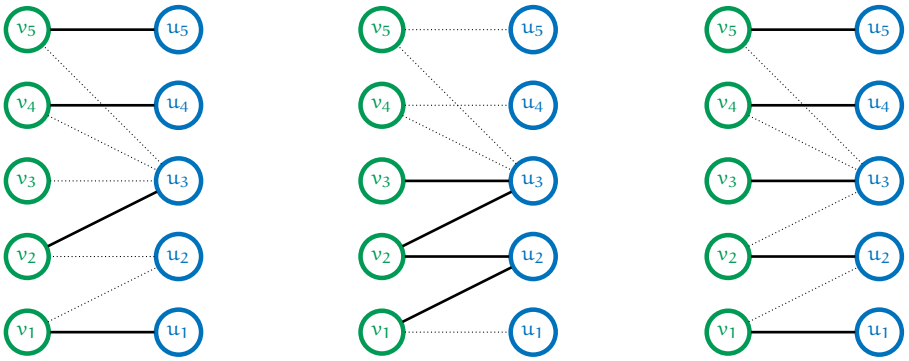

(a) A given matching M is depicted with thick black lines.

(b) In black thick line, an augmenting path for the matching M of figure 9a.

(c) The resulting augmented matching, in black thick line, is also perfect.

Figure 9: The procedure to increase the size of a matching.

Definition 2 (Augmenting path)**.** An alternating $(u_1 - v_r)$-path is called an *augmenting path* (for a certain matching M) if $(u_1, v_r) \notin M$.

We now have a strategy to increase the cardinality of our matching: we simply take the symmetric difference between the given matching M and an augmenting path for M constructed in some convenient way, as figure 9 shows. The matching M' constructed in this way clearly satisfies $|M'| = |M| + 1$, and one could proceed until a perfect matching is reached.

2.3.2 The Jonker-Volgenant algorithm

The Jonker-Volgenant (JV) algorithm of Jonker and Volgenant, 1987 is a primal-dual type algorithm (such as the Hungarian algorithm) in which optimality is obtained by a shortest-augmenting path subroutine based on the algorithm of section 2.2.2. The dual of linear problem 9 is realized as follows: one considers two sets of n variables, called the *dual* variables, $\{u_i\}_{i=1}^n$ and $\{v_j\}_{j=1}^n$, and searches for

$$\begin{aligned} &\max \sum_{i=1}^{n} u_i + \sum_{j=1}^{n} v_j \\ \text{under constraints} \quad & u_i + v_j \leqslant c_{ij} \qquad i, j = 1, \dots, n \\ & u_i, v_j \in \mathbb{R} \qquad i, j = 1, \dots, n \end{aligned} \tag{10}$$

By demanding that $x_{ij}(c_{ij} - u_i - v_j) = 0$ for $i, j = 1, \dots, n$ (known as the *complementary slackness condition*) one can iteratively update the dual variables with a transformation T in such a way that, $\forall \pi$

$$\sum_i c_{i\pi(i)} = \sum_i (c_{i\pi(i)} - u_i - v_{\pi(i)}) + \phi(T)$$

At optimality $\phi(T)$ is the desired value. For example, in the classical Hungarian algorithm of Kuhn, 1955 T is the row and column reduction procedure.

Following the extensive survey on linear assignment problems of Burkard and Çela, 1999 it is possible to describe the flow of this algorithm as follows.

1. Find an appropriate initial couple of primal (9) and dual (10) solutions respecting the complementary slackness condition.
2. Update the dual variables by constructing an augmenting path. At step i the actual augmenting path is the minimum length augmenting path in the shortest path tree obtained with a clever implementation of 2.2.2, and it joins an unassigned row to an unassigned column.
3. In the worst case scenario, i.e. without a careful choice of the initial primal-dual couple, step 2 iterates n times.

2.4 IMPLEMENTATION AND FEATURES OF THE CODE

Disordered statistical mechanics numerical studies have to do with average properties. It is clear that this may be pursued with at least numerically with a Monte Carlo approach, where a core program solves an instance of the problem at hand where the disorder is fixed, storing its output on some shared file. Only later the relevant means on quenched disorder are obtained, possibly thanks to some degree of parallelization.

The strongly sequential nature of algorithm Jonker and Volgenant, 1987 ruled out a single processing unit level parallelization, such the ones involving a CUDA/OpenCL implementation for GPU computing.

In this particular case this kind of solutions proved unpractical essentially for two reasons:

- The steps described in 2.3.2 must be executed by the same logical processor, requiring a very high computational power per core. This is not the case for a typical GPU computing unity.
- At high sizes a single instance of the program operates on $\sim 10^8$ numbers during the lapjv phase. Data storing in this step requires a very high amount of memory (of order 10 GB for $N \sim 2 \cdot 10^4$).

In order to obtain parallelization at least at the machine level it was chosen to splice up the code (679 lines of code in total) in three main utilities:

1. The main program, written in C++ and containing a fully self-consistent implementation of code Jonker and Volgenant, 1987 that accepts input parameters specific to the problem at hand and print outputs on simple text files, their names containing parameters values for future analysis. It can be easily tweaked if different ways of filling the cost matrix are required.

```
//Input from command line
startdim = atoi(argv[1]);
enddim = atoi(argv[2]);
step=atoi(argv[3]);
float P = atof(argv[4]);

//Strings construction
std::string temp;
std::string p = std::to_string(P);
temp = "Results/"+p+"-";
std::string results;
std::string times;
times = temp + "time.dat";
char const *p_timings = times.c_str();
```

Listing 2.1: Extract from main.cpp. The program accepts parameters from command line and gives proper names to outputs for future convenience.

2. The analysis routine, also written in C++, with the same input parameters ability as before, whose output is, according to input specifications, common statistical operations on big sets of numbers (mean, variance..). All this numbers are managed through a special class called "Statistica".

```
double tmp=0;
Statistica aggregator;//Simple constructor for obj

if (input.is_open()) { //input's an ifstream from stdl
  while (!input.eof()) {
    input >> tmp;
    aggregator.add(tmp);//methods for mean etc are private
      }
    }
input.close();
```

Listing 2.2: File reading happens with a simple cycle thanks to a specific method of the object Statistica.

3. A script written in BASH that conveniently calls the two previous programs. This script controls every input parameter of the main, such as the dimension of the space in problem EBMP, but also the Monte Carlo side, i.e. the number of instances to be computed at fixed parameters.

```
#! /bin/bash

INST=1000     #Number of instances of the problem
NSTART=2000   #Starting size
NFINISH=5000 #Target size
STEP=1000     #Step

for ((D=1; D<=10; D++)) #Dimension of the space - EBMP
  do
  for ((d=1; d<=INST; d++))
      do
    ./lapjv ${NSTART} ${NFINISH} ${STEP} ${D} ${D}
      echo -en 'Work in progress with D=P='${D}' ..'  $((
    100*${d}/${INST} )) '% done. \r'
      done

  for((k=NSTART; k<=NFINISH; k+=STEP))
    do
    ./analisi ${k} ${D} ${D}
    done
  done
```

Listing 2.3: The script that controls execution can be also be fed by command line.

This approach proved particularly effective because it was possible to execute the program on the cluster with shared filesystem LCM in Milan's Physics department.

In this setting one can concurrently execute the program on different nodes at fixed parameters, the output being written on the "same"

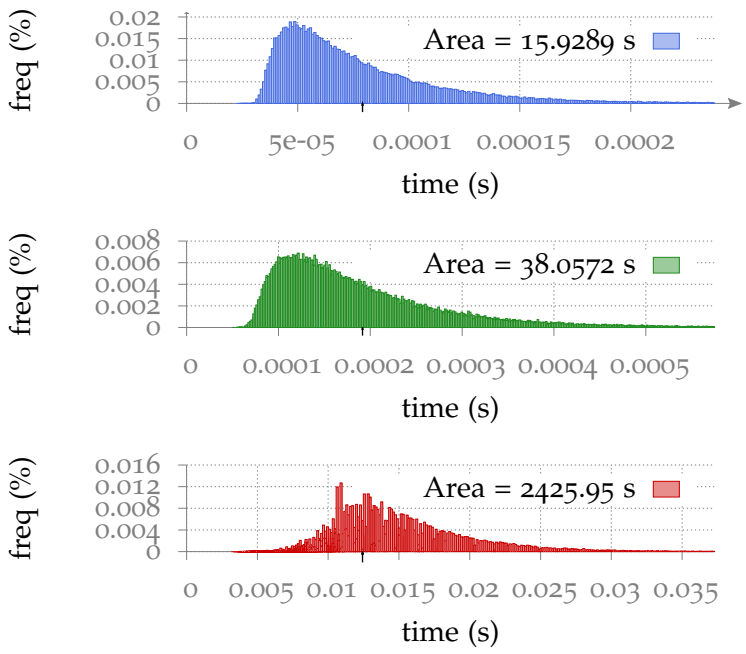

Figure 10: Distribution of execution times at sizes n=50 (blue), n=75 (green) and n=500 (red). Each histogram has 10^5 entries and the mean execution time is signaled by a small black arrow.

file with no more actions needed. Aggregation is done at the end of computation, when all running instances of the program have been completed by the nodes involved.

Coming to benchmark, a set of numerical tests were performed on the same machine, mounting an Intel Q9550 working at 2.83 GHz with 4GB of RAM.

The focus here is on the distribution of execution times at fixed parameters (a measure of how well the algorithm runs near his best-case execution) and of course on algorithm complexity. Having the physical model in mind these aspects are far from trivial: one expects for example a performance degradation in presence of high degeneracy, such as for $P = 1$ in the one dimensional EBMP, where a lot of comparisons are necessary during the augmentation phase.

This survey has shown some features that is worth visualizing and discussing.

First, the distributions of execution times at fixed parameters (such the ones in figure 10) is well unbalanced in his left tail, showing that the majority of executions stops near the best scenario, at least when the matrices size is < 500. These unbalanceness seems to gradually disappear at increasing n.

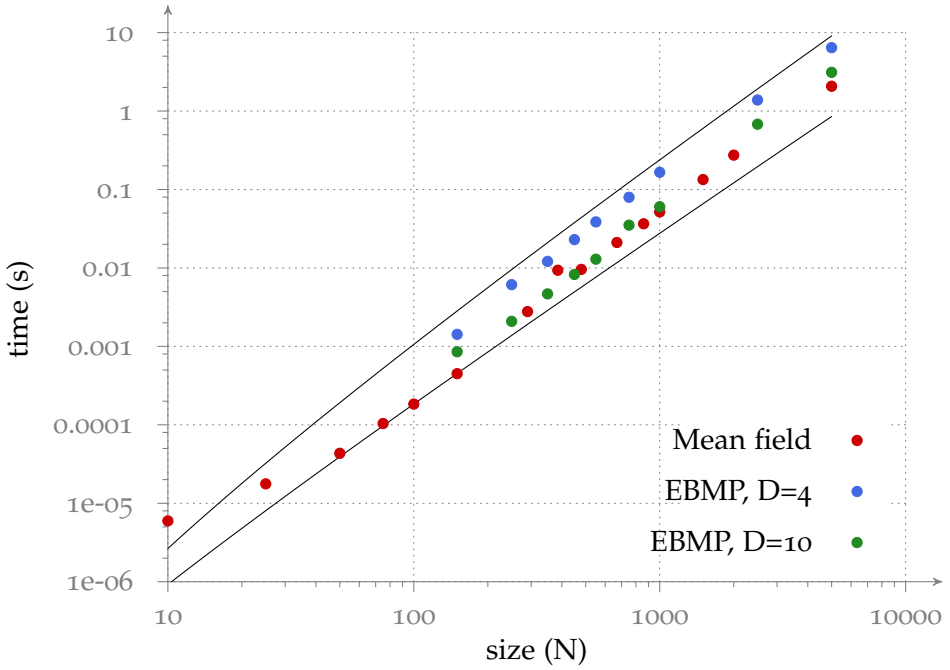

Figure 11: Average execution time as a function of the size N in three typical scenarios encountered in the work.

Second, the average time per execution (figure 11) stands between $O\left(N^2 \log N\right)$ and $O\left(N^3\right)$ throughout the accessible range, showing that, at least in the class of matrices involved in these kind of problems, this algorithm runs faster than the classical Hungarian algorithm Kuhn, 1955 (see Burkard and Çela, 1999 for a survey).

It emerged also that an instance of the frustrated (or Euclidean) model –blue and green points in figure 11– is completed in general slower than the completely random problem –the red points–, the performances improving at increasing dimensions; the upper black line is $t = 2.8 \cdot 10^{-11} N^3$.

3 RANDOM ASSIGNMENT VS EUCLIDEAN BIPARTITE MATCHING

Contents

3.1 INTRODUCTION

As noted in the previous section, where the formulation is completely general, a single specific instance of an assignment problem is completely defined by the cost matrix w. Of course in a number of applications the cost matrix has an experimental origin. For example, in the scheduling of a switcher with n inputs and n outputs, it is useful to assign inputs to outputs in order to minimize latency. In this case the cost matrix is given by the switch's manufacturer.

In this way, making an analogy with the objective function of eq (8), it is possible to speak about a *total cost* of the assignment (S_n is the symmetric group on n elements)

$$C_n(\pi; w) = \sum_{i=i}^{n} w_{i\pi(i)} \qquad \pi \in S_n \tag{11}$$

that has the meaning of an "energy". Thus a partition function can be defined as

$$Z_n(\beta; w) = \sum_{\pi \in S_n} e^{-\beta \sum_{i=1}^{n} w_{i\pi(i)}} \tag{12}$$

where, upon explicitation of the sum over the $n!$ configurations, there is no entropy term. Moreover, to elucidate that (12) depends on the "frozen" disorder w, a semicolon is used. We may summarize all numerical investigations of this thesis work in the study of what happens to (11) when $n \to \infty$ (the 'thermodynamic limit'). This thesis work focused on two problems:

RANDOM ASSIGNMENT PROBLEM

Consider a random variable η uniformly distributed in $[0, 1]$. Denoting its density by $\rho_\eta(y) = \chi_{[0,1]}(y)$, the r.v. $x = \eta^q$ has density

$$\rho_q(x) = \begin{cases} \frac{1}{q} x^{\frac{1}{q}-1} \chi_{[0,1]}(x) & \text{if } q > 0 \\ \delta(x-1) & \text{if } q = 0 \\ \frac{1}{q} x^{\frac{1}{q}-1} \chi_{[1,+\infty)}(x) & \text{if } q < 0 \end{cases} \tag{13}$$

The "random assignment problem" deals with studying what happens under these assumptions to (11) in the $n \to \infty$ when each of the entries of the weight matrix w_{ij} is a random variable with density (13).

Differently stated, given a complete bipartite graph $K_{n,n}$, we are assigning each of its n^2 links a random weight with density (13) and searching for the minimal total weight perfect matching as well as corrections to this scaling regime as $n \to \infty$.

Comparing results with literature, it is convenient to define the *exponent*

$$r = \frac{1}{q} - 1 \tag{14}$$

This equation admits an interesting generalization as shown in eq. (3.5.1).

Adopting this convention, density (13) has finite moments for $r \geqslant -1$ ($\forall q \geqslant 0$), while, when $r < -1$ ($q < 0$), the highest defined moment is the n-th, with $n = \lfloor -(r+1) \rfloor$. In this way, where defined, the moment generating function is

$$\widetilde{\rho}_r(k) = \mathbb{E}[e^{xk}] = \sum_{n=0}^{\infty} \frac{r+1}{n+r+1} \frac{k^n}{n!} \equiv {}_1F_1(r+1; r+2; k) \tag{15}$$

EUCLIDEAN BIPARTITE MATCHING PROBLEM

Euclidean Bipartite Matching Problem (EBMP) is a linear assignment problem where the focus is placed on matching n points of a certain type $\{\mathbf{b}_i\}_{i=1}^n$(the "blacks") to n points of another type $\{\mathbf{w}_j\}_{j=1}^n$ (the "whites").

In particular blacks and whites form the partite sets of $K_{n,n,}$ and are all randomly distributed in some Euclidean space.

In graph theoretical terms, we are moving the randomness from links to vertices. Again one studies the scaling behavior of some optimal configuration, the difference being that this disordered system is also frustrated (for example by the triangular inequality).

In this work all points are chosen uniformly in the D-dimensional hypercube of side 1 C_D, or in the D-dimensional torus $\mathbb{T}^d$. Each of these two cases is completely specified by choosing the metric.

More precisely, the D coordinates of a point are r.v. with density

$$\rho_{x_i}(y) = \chi_{[0,1]}(y) \tag{16}$$

and the distance $d(\mathbf{b}_i, \mathbf{w}_j)$ between point $\mathbf{b}_i$ and the point $\mathbf{w}_j$ is

$$\sqrt{\sum_{k=1}^{D} \left(\min\left\{|(b_i)_k - (w_j)_k|, 1 - |(b_i)_k - (w_j)_k|\right\}\right)^2} \text{ on } \mathbb{T}^D$$

$$\sqrt{\sum_{k=1}^{D} \left((b_i)_k - (w_j)_k\right)^2} \text{ on the hypercube } C_D = X_{i=1}^{D}[0,1] \tag{17}$$

In the EBMP the general cost matrix appearing in (11) is completely specified by

$$w_{ij} = d(\mathbf{b}_i, \mathbf{w}_j)^P \tag{18}$$

In this problem it is interesting to study expression (11) in the thermodynamic limit $n \to \infty$.

3.2 RANDOM ASSIGNMENT PROBLEM

3.2.1 Background

The possibility to deal with a combinatorial optimisation problem using methods borrowed from the statistical mechanics of disordered systems was first exploited in the pioneering article Mézard and Parisi, 1985, where the random monopartite matching problem is studied. This problem is very similar to RAP, except for the fact that all the $2n$ points belong to the same class.

As stated in the ach matching of the complete graph $\mathbb{K}_{2N}$ has an energy depending on the realization of the frozen disorder; among the many interesting questions about properties of optimal configurations, one may be interested in the configuration realizing the ground state level, or its energy.

In complete analogy with eq. (13)) the energy of a matching is defined as

$$E\left(\{n_{ij}\}\right) = \sum_{1\leqslant i<j\leqslant 2N} n_{ij} l_{ij} \tag{19}$$

where, in Mézard and Parisi convention, l_{ij} has density $\rho(x) = \frac{x^r e^{-x}}{r!}$. By expliciting the matching constraint the partition function is

$$\begin{aligned} Z(\beta, N; l) &= \sum_{\{n_{ij}=0,1\}} \left(\prod_{i=1}^{2N} \delta(1 - \sum_{j=1}^{2N} n_{ij}) \right) e^{-\beta E(\{n_{ij}\})} \\ &= \sum_{\{n_{ij}=0,1\}} \prod_{i=1}^{2N} \left(\int_0^{2\pi} e^{i\lambda_i (1 - \sum_{j=1}^{2N} n_{ij})} \frac{d\lambda_i}{2\pi} \right) e^{-\beta E(\{n_{ij}\})} \\ &= \prod_{i=1}^{2N} \left(\int_0^{2\pi} \frac{d\lambda_i}{2\pi} e^{i\lambda_i} \right) \prod_{j<k} \left(1 + e^{-\beta l_{jk}} e^{-i(\lambda_j + \lambda_k)} \right) \\ &= \prod_{i=1}^{2N} \left(\int_0^{2\pi} \frac{d\lambda_i}{2\pi} e^{i\lambda_i} \right) \left(1 + \sum_{j<k} u_{jk} + \sum_{\substack{j<k \\ l<m}} u_{jk} u_{lm} + \dots \right) \end{aligned} \tag{20}$$

where:

- from the second to the third line the integral representation of the δ function has been introduced and the sum over the configurations has been performed

- from the third to the fourth line the definition

$$u_{ij}(\beta) \equiv e^{-\beta l_{ij} - i(\lambda_i + \lambda_j)} \tag{21}$$

has been introduced.

Before proceeding any further some comments are in order.

1. It is possibile to define an energy density for this model, hoping that its thermodynamic limit is independent of the particular disorder realization

$$f(N) = N^{\frac{1}{r+1}-1} F(\beta(N)) \tag{22}$$

   To ensure the existence of a non trivial thermodynamic limit it is necessary that the inverse temperature satisfies $\beta = \hat{\beta} N^{\frac{1}{r+1}}$.

   Even if, as stated in Houdayer et al., 1998, it can be proven that the distribution of (22) peaks around some value when $N \to \infty$, this is not sufficient to prove convergence in probability. Indeed, to prove self-averageness, it has to be proven that (22) tends in probability to a constant independent of the realization, depending at most on the parameter r;

2. it is the behavior of disorder's distribution near the origin that fully determines the limit value of the average optimal cost at zero temperature. A simple argument of proximity shows that the typical nearest neighbor can be found at distance $\frac{1}{N^{\frac{1}{r+1}}}$.

   Hence there is no difference in choosing such distribution as a uniform r.v. on $[0,1]$ or as an exponential r.v. with intensity 1, as in fact it has been done. Of course, the precise choice of disorder distribution is relevant at finite N.

The computation may be sketched as follows. In the so called *replica method* one computes the free energy via the identity

$$\log x = \lim_{n \to 0} \frac{x^n - 1}{n} \tag{23}$$

By substituting $x = Z$ and integrating over $\rho(l_{ij})$ the averaged free energy (i.e. left hand side of equation (23)) can be computed directly as the limit $n \to 0$ of a system of n non-interacting replicas (from the Latin *replicare*, to "fold once again") of the initial system.

To see how this happens consider the expression

$$Z^n(\beta, N; l) = \prod_{a=1}^{n} \prod_{i=1}^{2N} \left(\int_0^{2\pi} \frac{d\lambda_i^a}{2\pi} e^{i\lambda_i^a} \right) \prod_{a=1}^{n} \left(1 + \sum_{j<k} u_{jk}^a(\beta) + \dots \right) \tag{24}$$

where now for each of the n replicas it has been defined the quantity

$$u_{ij}^a(\beta) \equiv e^{-\beta l_{ij} - i(\lambda_i^a + \lambda_j^a)} \tag{25}$$

Since the average of (24) with respect to disorder distribution factorizes on each link

$$\int_0^\infty dl_{ij} \frac{l_{ij}^r}{r!} e^{-l_{ij}} \prod_{a=1}^{n} \left(1 + u_{ij}^a(\beta)\right) = 1 + \frac{1}{N} \sum_{s=1}^{n} \frac{1}{\left(\hat{\beta} s\right)^{\frac{1}{r+1}}} \sum_{\substack{a_1, \dots a_s = 1 \\ a_1 \leqslant \dots \leqslant a_s}}^{n} \prod_{r=1}^{s} u_{jk}^{a_r} \tag{26}$$

so that it can be performed to give

$$\overline{Z^n(\beta,N;l)} = \int \prod_{s=1}^{n} \prod_{a_1<\ldots<a_s} \frac{dQ_{a_1\ldots a_s}}{\mathcal{N}(s,N)} \cdot \\ \cdot e^{N\left(-\frac{1}{2}\sum_{s=1}^{n}(s\hat{\beta})^{r+1}\sum_{a_1<\ldots<a_s} Q^2_{a_1\ldots a_s} + 2F(1,Q)\right)} \tag{27}$$

where $\mathcal{N}(s,N)$ is a proper normalization constant coming from gaussian integration and $F(1,Q)$ is the free energy associated to the partition function at temperature one

$$z(1,Q) = \prod_{a=1}^{n}\left(\int_0^{2\pi}\frac{d\lambda_i^a}{2\pi}e^{i\lambda_i^a}\right) e^{\sum_{s=1}^{n}\sum_{a_1<\ldots<a_s} Q_{a_1\ldots a_s} e^{-i(\lambda^{a_1}+\ldots+\lambda^{a_s})}} \tag{28}$$

The saddle point equation for eq. (27) ($N\to\infty$) is

$$Q_{a_1\ldots a_s} = \frac{2}{(s\hat{\beta})^{(r+1)}}\left\langle e^{-i(\lambda^{a_1}+\ldots+\lambda^{a_s})}\right\rangle_z \tag{29}$$

where $\langle\ldots\rangle_z$ is the average with respect to partition function (28).

The *replica symmetry hypothesis* consists in assuming that tensor Q satisfies $Q_{a_1\ldots a_s}\equiv Q_s$. By defining

$$\Psi_r(\eta) = \sum_{s=1}^{\infty}(-1)^{s-1}\frac{Q_s e^{s\eta}}{s!} \tag{30}$$

the saddle point equation may be written in term of $\Psi_r(\eta)$. In the $\hat{\beta}\to\infty$ limit the free energy density is

$$E_r|_{T=0} \underset{\beta\to\infty}{=} (r+1)\int_{-\infty}^{+\infty}\Psi_r(s)e^{-\Psi_r(s)}\,ds \tag{31}$$

where Ψ_r satisfies the following integral equation

$$\frac{\Psi_r(\eta)}{2} = \int_0^{+\infty}\frac{s^r}{r!}e^{-\Psi_r(s-\eta)}\,ds \tag{32}$$

In case $r=0$ an exact solution is possible. Indeed differentiating twice equation (32) with respect to η shows that $\Psi_0''(\eta)$ is an even function satisfying

$$\Psi_0''(\eta) = \Psi_0'(\eta)\Psi_0'(-\eta) \tag{33}$$

on all $\mathbb{R}$. Thus $\Psi_0(x)+\Psi_0(-x)=c_1$ so that

$$\Psi_0'' = \Psi_0'(c_1-\Psi_0') \tag{34}$$

which, integrated one time from o to η gives

$$\Psi_0'(\eta)e^{\Psi_0(\eta)} = \Psi_0'(0)e^{\Psi_0(0)}e^{c_1\eta}$$

By defining the function $\phi_0(\eta) = e^{\Psi_0(\eta)}$, and integrating again

$$\phi_0(\eta) - \phi_0(0) = \frac{\phi_0'(0)}{c_1}\left(e^{c_1\eta} - 1\right)$$

Three relations are required to find the three unknowns. The first is

$$\frac{1}{2}\left(\Psi_0(\eta) - \Psi_0(-\eta)\right) = \int_{-\eta}^{\eta} e^{-\Psi_0(t)}\, dt = 2\eta e^{-\Psi_0(0)} \tag{35}$$

so that

$$\begin{aligned}\frac{1}{2}c_1 \equiv & \frac{1}{2}\left(\Psi_0'(\eta) + \Psi_0'(-\eta)\right) \\ = & 2e^{-\Psi_0(0)}\end{aligned} \tag{36}$$

This constraint implies $\phi_0'(0) = 2$. The second and the third constraints come as a result from observing that

$$\phi_0''(0) = \phi_0'(0)^2$$

a relation that implies $c_1 = \phi_0'(0)$. Indeed, inserting $\Psi_0(\eta) = \log \Phi_0(\eta)$ in (35) fixes also $\Phi(0) = 2$. In conclusion

$$\Psi_0(\eta) = \log \phi_0(\eta) = \log(1 + e^{2\eta})$$

In this way the ground state energy can be computed exactly. It is

$$\begin{aligned}E_0|_{T=0} = & \frac{1}{2}\int_0^{+\infty} \frac{s}{e^s - 1}\, ds \\ = & \frac{1}{2}\sum_{n=0}^{+\infty}\int_0^{+\infty} e^{-(n+1)s} s\, ds \\ = & \frac{1}{2}\sum_{n=0}^{+\infty} \frac{d}{dn}\frac{1}{n+1} e^{-(n+1)s}\Big|_0^{+\infty} \\ = & \frac{1}{2}\sum_{n=0}^{+\infty} \frac{1}{(n+1)^2} = \frac{\pi^2}{12}\end{aligned} \tag{37}$$

This last computation is very similar to the ones emerging in the study of the specific heat of solids, for example in the Debye model at low temperature.

At the end of Mézard and Parisi, 1985 is also observed that, by applying the same method of resolution on the bipartite case –which is the case studied in this work– very similar calculations are obtained, the relevant ground states energies being $2^{\frac{1}{r+1}}$ times larger.

In the RAP context it is placed a famous conjecture (Parisi, 1998) about the average optimal at a finite size n, when quenched disorder is distributed exponentially with mean 1. This appealing conjecture stated that

$$\langle C_n(\pi^*)\rangle = \zeta_n(2) \equiv \sum_{k=1}^{n} \frac{1}{k^2} \tag{38}$$

where $\zeta_n(s)$ is the truncated Riemann zeta function.

Looking into the state of the art about random links problem, in Brunetti et al., 1991 both the monopartite and bipartite matching problems are considered, with numerical results for both averaged optimal cost and finite size correction, confirming to very high precision the predictions of the original article mentioned above.

An extensive numerical investigation on the RAP is Lee and Orlin, 1993: thanks to an algorithm called "QuickMatch", based on the algorithm of section 2.2.2, they were able to compute the optimal matching on $K_{2\cdot10^6,2\cdot10^6}$, and on a bipartite graph with as much as 10^{12} edges.

Another previous analysis of the random monopartite and bipartite matching problem is the already mentioned one Houdayer et al., 1998, where also a power law distribution of the type (13) for costs is assumed (apart from a normalization that will be discussed later, remind that $d = r + 1$). In this work a comparison of the distribution of costs in the mean optimal configuration in both monopartite and biparite case is presented.

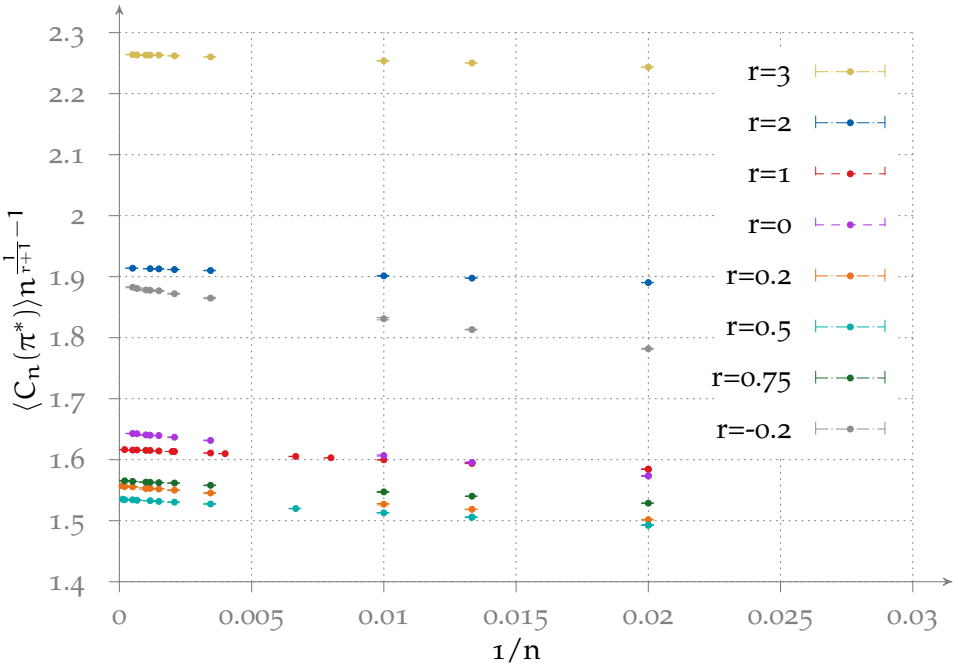

Figure 12: Each point in this figure is the mean value of at least 10^4 simulations. As shown in the key, every color corresponds to a different RAP, each completely specified by the value of r. Extrapolation have been performed for every color via expression (39); it was possible to merge three different scales of the size of the system, n: $n \in S_1 = (10, 100)$, $n \in S_2 = (100, 1000)$, and $n \in S_3 = (1000, 12500)$. Notice that, since every straight line that fits points has negative slope, all coefficients of the $\frac{1}{n}$ corrections in (39) is negative.

3.2.2 Numerical findings

A huge amount of simulations has been performed in order to verify if the quantity defined in (22) peaks itself around some disorder independent limit, especially in the region $r < 0$, where no numerical value in the literature is available.

Consequently to the considerations made in 3.2.1 the fitting function is chosen as

$$n^{\frac{1}{r+1}-1}\langle C_n(\pi^*)\rangle = w_r\left(1 + \frac{A(r)}{n} + \frac{B(r)}{n^2}\right) \tag{39}$$

(recall that C_n is defined in (11), $\pi^* \in S_n$ realizes the minimum and $\langle\cdots\rangle$ is the sample mean over the disorder, distributed according to (13). After a proper rescaling, due to the different conventions found in the literature, a good agreement with is found, as resumed in table 1. These results, under the rescaling of a factor $2^{\frac{1}{r+1}}$ mentioned in the previous paragraph, matched also very well the one presented in Mézard and Parisi, 1988 for $r = 1$ and $r = 2$.

r	Lee and Orlin, 1993	Houdayer et al., 1998	w_r
0	1.64474	1.64536	1.64494(9)
1	1.61786	1.61718	1.61698(8)
2	1.9139	1.91474	1.91456(7)
3	2.2658	2.26455	2.26430(9)

Table 1: A pletora of different normalization conventions has been used to study the random assignment problem. This requires a proper rescaling of the coefficients involved–their meaning being discussed in section 3.5–. This done, agreement with previous numerical investigations is quite good.

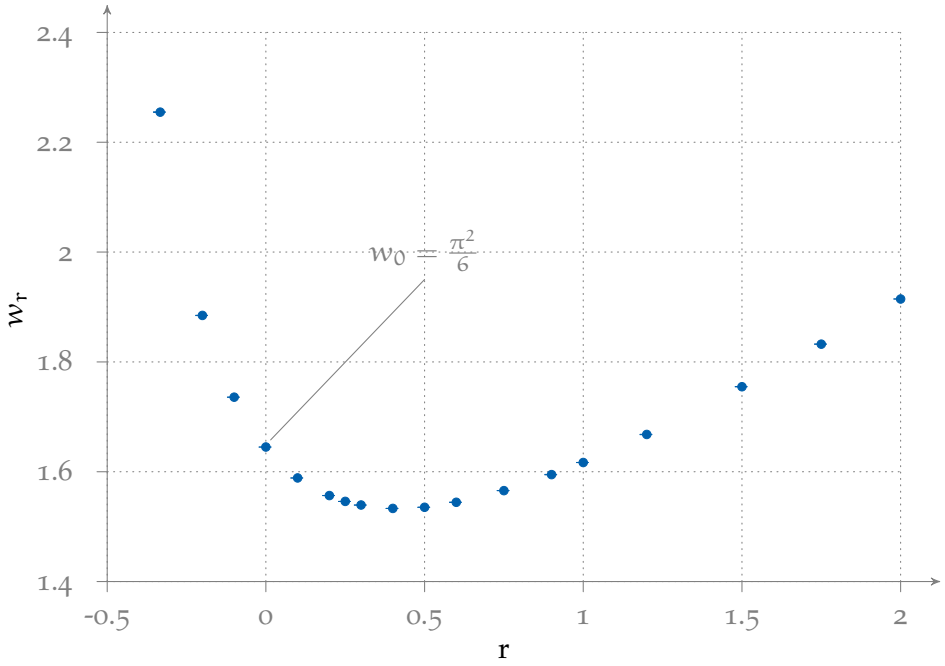

r	w_r
$-\frac{1}{3}$	2.2549(6)
-0.2	1.8846(3)
-0.1	1.7357(3)
0	1.64494(9)
0.1	1.5886(2)
0.2	1.5564(1)
0.25	1.5458(1)
0.3	1.5391(2)
0.4	1.5331(1)
0.5	1.53525(8)

r	w_r
0.6	1.5440(2)
0.75	1.5654(1)
0.9	1.5945(2)
1	1.61698(8)
1.2	1.6682(2)
1.5	1.7545(1)
1.75	1.8324(1)
2	1.91456(7)
2.5	2.0864(1)
3	2.26430(9)

Figure 13: All results obtained simulating RAPs. w_r is defined in eq. (39) and errors on the last digit is between parentheses.

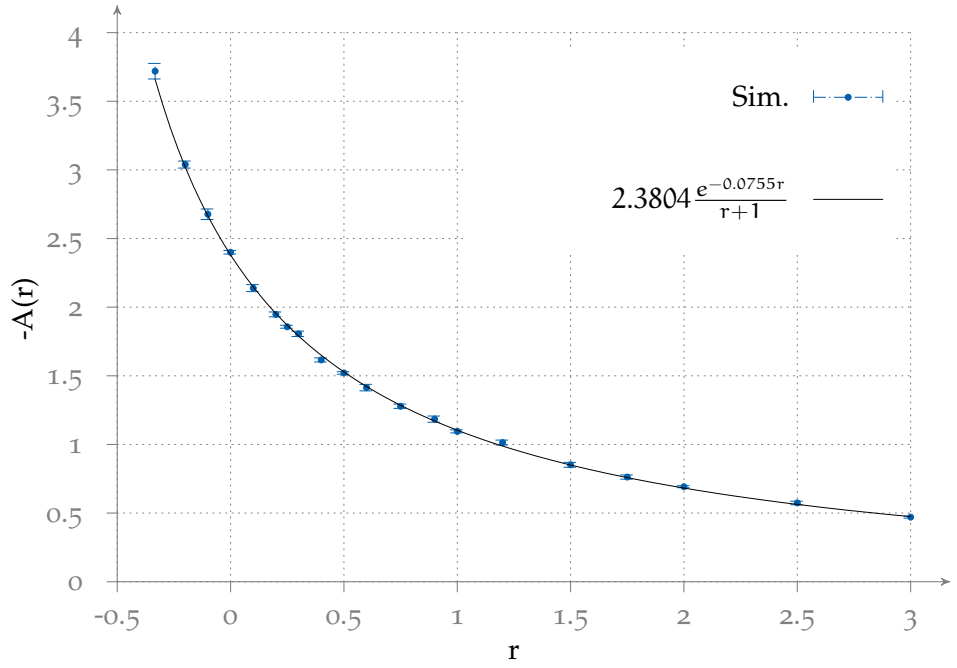

r	A(r)
$-\frac{1}{3}$	-3.71(5)
-0.2	-3.03(2)
-0.1	-2.68(4)
0	-2.40(1)
0.1	-2.14(2)
0.2	-1.95(2)
0.25	-1.85(1)
0.3	-1.80(2)
0.4	-1.61(1)
0.5	-1.52(1)

r	A(r)
0.6	-1.41(2)
0.75	-1.27(1)
0.9	-1.18(2)
1	-1.09(1)
1.2	-1.01(2)
1.5	-0.85(2)
1.75	-0.76(1)
2	-0.692(8)
2.5	-0.57(1)
3	-0.470(7)

Figure 14: All results obtained simulating RAPs. $A(r)$ is defined in eq. (39) and errors on the last digit is between parentheses.

With respect to the exponential fit for the coefficient $A(r)$ defined in (39) and presented in figure 14, it is worth noting that the point at $r = 3$ would have been improperly fitted without the exponential correction at numerator. However, since the exponent is really small (~ 0.0755), we cannot take out the chance that the expansion in r of numerator is finite.

To prove this two assumptions a simulation for very high values of r would be needed.

3.3 ONE DIMENSIONAL EUCLIDEAN BIPARTITE MATCHING PROBLEM

3.3.1 One dimensional case with open boundary conditions

Exact formulas for the convex case in both the interval $(0,1)$ and S^1 can be found in Caracciolo, Sergio and Sicuro, Gabriele, 2014, where it is shown that the average optimal cost can be computed as a particular expected value over the stochastic process called "Brownian bridge". This link allows also a study of the correlation functions in these cases.

The link with the Brownian bridge as well as properties of the optimal matching for both convex and concave cost are established as theorems in Boniolo et al., 2014; a continuum analogue of this problem in the framework of measure theory, called the *Monge-Kantorovich problem*, with strictly concave cost, has been studied previously in McCann, Robert, 1999. In the next section a brief summary of these results will be presented; a review of the general Monge-Kantorovich problem in measure theory is postponed to 3.4.

3.3.2 Some remark on the properties of the optimal matching for the EBMP in one dimension

In this section is presented a brief literature review of known results of the one dimensional Euclidean matching problem. These well established results were used to check consistency check of the code of section 2.4. Some possibly new –to the best of author's knowledge– numerical investigation in the concave $P \in [0,1]$ and negative $P \in [-1,0]$ cases are then discussed without the possibility to check their sensibleness.

Consider a particular realization of n whites and n blacks. Among the many ways in which we may visualize a matching, one is drawing n points in the first quarter of a Cartesian plane, one for each of the n arcs in the matching, its abscissa and ordinate being respectively the abscissa of the black and of the white point that define an arc. A convenient definition follows.

Definition 3. Given a particular matching $\pi \in S_n$ between n black points $\{b_i\}_{i=1}^n$ and n white points $\{w_j\}_{j=1}^n$, the *path of the matching* (or *matching path*) is the unique piece-wise linear function that passes through the points $P_i = (b_i, w_{\pi(i)}) \in \mathbb{R}^+ \times \mathbb{R}^+$, the n representatives of each arc composing a matching.

A *strictly convex cost* is a lower bounded function $c : \mathbf{D} \to \mathbb{R}$ that satisfies

$$c\left(tx + (1-t)y\right) < tc(x) + (1-t)c(y) \quad t \in [0,1]$$

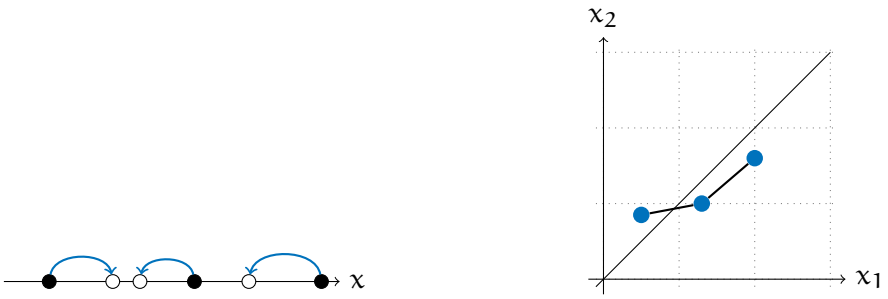

(a) A matching for $n = 3$

(b) The corresponding path

Figure 15: The *matching path* construction in the one dimensional convex case with open boundary conditions.

This property, which is true if and only if $c(x)$ has monotone increasing increments, provides a characterization of the optimal matching in the case $P > 1$ for cost (18) in $D = 1$.

Lemma 2. *An optimal matching for a strictly convex cost is non-decreasing, i.e. its associated matching path has positive difference quotients.*

Proof. On the contrary, suppose that a matching path has at least one of its pieces with negative slope, say $\frac{w_{i+1}-w_i}{b_{i+1}-b_i} < 0$, where b_i (resp. b_{i+1}) is matched to w_i (resp.w_{i+1}).

We may suppose without loss of generality that $b_i < b_{i+1}$, in which case necessarily $w_{i+1} > w_i$. In this way the two points $x_1 = b_i - w_{i+1}$ and $x_2 = b_{i+1} - w_i$ belong to the interval $(b_i - w_{i+1}, b_{i+1} - w_i)$; moreover, viewed as a convex combination of these two extrema, they are symmetric in the exchange $t \mapsto (1-t)$. By the strict convexity of the cost function follows that

$$c(b_i, w_{i+1}) + c(b_{i+1}, w_i) < c(b_i, w_i) + c(b_{i+1}, w_{i+1})$$

which shows that the matching is not optimal. □

Note that there is a one-on-one correspondence between changes of sign of $w_{\pi(i)} - b_i$ and crossing points between the respective matching path and $y = x$.

It is also clear that for costs of the type 18 the optimal solution is unique, since any exchange implies a negative difference quotient on its path, thus strictly raising the total cost; moreover, if we adopt the statistical mechanics picture, at fixed realization of the disorder –by the monotonicity of the function x^P– the optimal solution is the same $\forall P > 1$.

This lemma provides also a recipe that greatly simplifies the numerical analysis of one dimensional EBMPs: starting from a given realization of the disorder, it is sufficient to sort separately the n whites and the n blacks, the optimal solutions at every fixed instance is the one in which the leftmost black point is matched with the leftmost white

point (in the language of permutations, we're stating that the optimal map after sorting is the identity $\pi(i) = i$, $\forall i = 1, \dots, n$).

For example, in this thesis the sorting task is accomplished by the use of classical recursive "quicksort", a fact that lowers the computational complexity from $O(n^3)$ –worst case scenario of algorithm of section 2.3.2– to $O(n \log n)$, allowing the simulation of systems of size up to 10^8.

In the case with open boundary conditions and strictly convex cost it was showed in Boniolo et al., 2014 that it is possible to proceed even further: in the so-called "grid-Poisson" setting, the n white points are fixed at positions $\frac{i}{n}$, $i = 1, \dots, n$ while the blacks are again uniformly chosen at random.

In the g-P EBMP the probability for the i-th black to be found in the interval $[y, y + dy]$ is

$$P(y_i \in dy) = \binom{N}{i} y^i (1-y)^{N-1} \frac{i}{y} dy$$

The rescaled distance of a black to its optimally matched white

$$\mu(y) := \frac{i}{\sqrt{n}} - \sqrt{n} y \tag{40}$$

in the thermodynamic limit $n \to \infty$, as proved in Caracciolo, Sergio and Sicuro, Gabriele, 2014, is distributed according to

$$\rho(\mu(y)) = \frac{1}{\sqrt{2\pi y(1-y)}} e^{-\frac{\mu^2}{2y(1-y)}} d\mu$$

which is the distribution of the Gaussian stochastic process called the Brownian bridge B_y with $y \in [0, 1]$ (see A.2.1 for a brief review of its properties). Defining now

$$\Phi(x) = \frac{2^x}{\sqrt{\pi}} B(x+1, x+1) \Gamma\left(x + \frac{1}{2}\right) \tag{41}$$

where $B(x, y)$ and $\Gamma(x)$ are the usual Euler's Beta and Gamma functions, the mean cost averaged over the disorder $\langle C \rangle$ is given by

$$\mathbb{E}|\mu(y)|^P = n^{-\frac{P}{2}} \Phi\left(\frac{P}{2}\right) \qquad P > 1$$

It is worth noticing that, when $P \leqslant 1$ (not strictly convex case) the optimal matching is in general not ordered (i.e. the corresponding matching path fails to be non-decreasing), preventing the construction of a transport field of the type $\mu(y)$ of eq. (40). Already at fixed disorder realization the optimal matching is qualitatively very different from the optimal matching that realizes the minimum in the strictly convex case. The following lemma, as the previous one, is inspired by analogue results in the continue transport theory in McCann, Robert, 1999, and shows some property of the optimal matching in the strictly concave case.

Lemma 3. *If the cost c is an increasing strictly concave function*

$$c\,(tx + (1-t)y) > tc(x) + (1-t)c(y) \quad t \in [0,1]$$

the following two properties hold:

- *the optimal matching is uncrossing.*
- *the optimal matching satisfies the "rule of three", that is, in a nested configuration whose matching path crosses $y = x$ a certain area is forbidden.*

Proof. The uncrossing property of the optimal matching is exactly what is expected by linking the points in the configuration, ad done in 16a; this property can be proved with an argument completely analogue to the one used in lemma (2).

To state and prove the rule of three consider figure 16a, which catch the possible nested matchings with reverse order of the arrow: these are the two only possible orderings that are both uncrossing and incident with the bisector (in the sense that their matching path does intersect $y = x$). Assume $b_j \leqslant w_{\pi(i)} < b_i \leqslant w_{\pi(j)}$ (as the blue couple of matchings in figure 16a) is optimal. Obviously $c(b_i, w_{\pi(i)}) = c(b_i, 2b_i - w_{\pi(i)})$, but, since the cost is increasing, it is also clear that $c(b_j, w_{\pi(i)}) < c(b_j, 2b_i - w_{\pi(i)})$. In this way from the optimality condition follows

$$c(b_j, 2b_i - w_{\pi(i)})) + c(b_i, w_{\pi(i)}) < c(b_i, w_{\pi(j)}) + c(b_j, 2b_i - w_{\pi(i)}))$$

Necessarily $b_j < 2b_i - w_{\pi(i)} < w_{\pi(j)}$ (otherwise the two blue arrows in the figure would cross violating the uncrossing rule). With the same argument one proves the other possibility, namely $b_j < 2w_{\pi(i)} - b_i < w_{\pi(j)}$ □

In McCann, Robert, 1999 the last part of this lemma is pictorially stated as follows: if one considers the two circles $O(w_{\pi(i)}, b_{\pi(i)})$ and

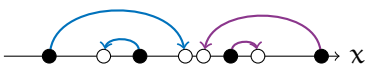

(a) A matching for $n = 4$ exhibiting nesting.

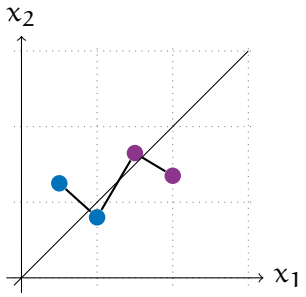

(b) The matching path corresponding to 16a.

Figure 16: If arc A is nested in arc B, then A's representative point is closer to $y = x$ than B's.

$O'(w_{\pi(j)}, b_{\pi(j)})$ having respectively $w_{\pi(i)}$ and $b_{\pi(i)}$ ($w_{\pi(j)}$ and $b_{\pi(j)}$) as antipodal points, in the optimal matching if $O'(w_{\pi(j)}, b_{\pi(j)})$ encloses $O(w_{\pi(i)}, b_{\pi(i)})$, then it encloses also the circle

$$O''(2b_i - w_{\pi(i)}, 2w_{\pi(i)} - b_{\pi(i)})$$

whose diameter is three times the diameter of $O'(w_{\pi(j)}, b_{\pi(j)})$.

It is possible to look at the construction of the matching path of the optimal configuration also in a "dynamical way". Starting from a certain point of the path $P_t = (x_t, y_t)$, where is it possible to find the next one $P_{t+1} = (x, y)$ in the optimal matching?

In the convex case the answer to this question is simple: since the matching path is non-decreasing, it is

$$P_{t+1} \in \mathbb{H}_+, \quad \mathbb{H}_+ = \{(x, y) \in [0,1] \times [0,1] \,|\, x - x_t \geqslant 0 \wedge y - y_t \geqslant 0\}$$

i.e. the blue shaded area across $y = x$ in figure 17. It is readily seen that $\forall t$ this rectangular accessible region, which is also simply connected, is uniquely identified by the *actual* position of P_t.

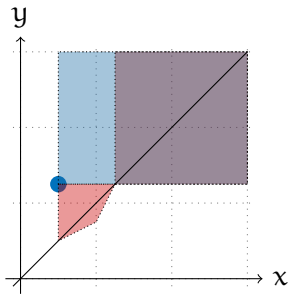

Figure 17: The accessible region for an optimal configuration in the convex case (the light blue rectangle $[0.5, 3] \times [1.25, 3]$) differs from the accessible region in the concave case (quadrilateral accross the bisector $\cup [1.25, 3] \times [1.25, 3]$, both shaded in red).

On the contrary in the concave case a different situation occurs. The two constraints of lemma 3 are non local, in the sense that the accessible region for P_{t+1} given P_t "splits up" in two disconnected sub regions, one accessible if the arc which P_{t+1} represents is outside the arc represented by P_t, and the other if it is instead nested inside, so that the accessible region is not simply connected.

3.3.3 Numerical results in the one-dimensional case

The quality of numerical investigation in the convex case with OBC was checked against analytic predictions of eq. (41), both using and non-using the ordering trick described in the previous section. This test confirmed also very well that the average optimal cost scales as $n^{-\frac{p}{2}}$ when $n \to \infty$, as it should be by the Brownian bridge correspondence, while a different asymptotic beahvior for these quantities is strongly supported by numerics in regions of the space of parameters where analytic predictions are not available[1].

In particular in the concave ($p \in [0,1]$) and negative ($p \in [-1.1, 0]$) cases there is strong numerical evidence for a deviation of the scaling exponent of the optimal cost averaged over the disorder from the convex regime. The extrapolation of the data is done via the relation

$$C_p \sim \left\langle C_n^{(p)} \right\rangle n^{\epsilon+\frac{p}{2}-1} \qquad n \to \infty \tag{42}$$

the value of ϵ representing the deviation from the convex case; the results, which are collected in table 2 and plotted in figure 18, are obtained with a simple fit, whereas each value at fixed n is the mean of at least 10^4 realizations of the disorder.

p	C_p	ϵ	p	C_p	ϵ
-1.1	2.17(1)	0.552(1)	0.1	0.927(2)	0.0474(3)
-0.9	1.887(2)	0.4517(2)	0.2	0.879(5)	0.0908(8)
-0.75	1.702(4)	0.3767(4)	0.3	0.811(7)	0.121(1)
-0.5	1.422(3)	0.2507(4)	0.4	0.777(8)	0.147(2)
-0.4	1.325(1)	0.2005(1)	0.5	0.714(1)	0.155(3)
-0.3	1.235(2)	0.1504(2)	0.6	0.627(1)	0.149(3)
-0.2	1.148(1)	0.10006(5)	0.75	0.489(5)	0.104(2)
-0.1	1.0728(2)	0.05013(2)	0.9	0.376(5)	0.044(1)

Table 2: Summary of the results for $p \in [-1.1, 11]$.

p	C_p	$\Phi\left(\frac{p}{2}\right)$
1	0.321(3)	0.313328
1.1	0.288(1)	0.289102
1.5	0.217(1)	0.218591
2	0.167(1)	0.166666
3	0.1175(5)	0.117498
5	0.096(3)	0.097915
7	0.123(5)	0.128513
11	0.55(3)	0.530118

1 Except from the results for correlation functions when $p \in [0.75, 1]$ presented in Boniolo et al., 2014).

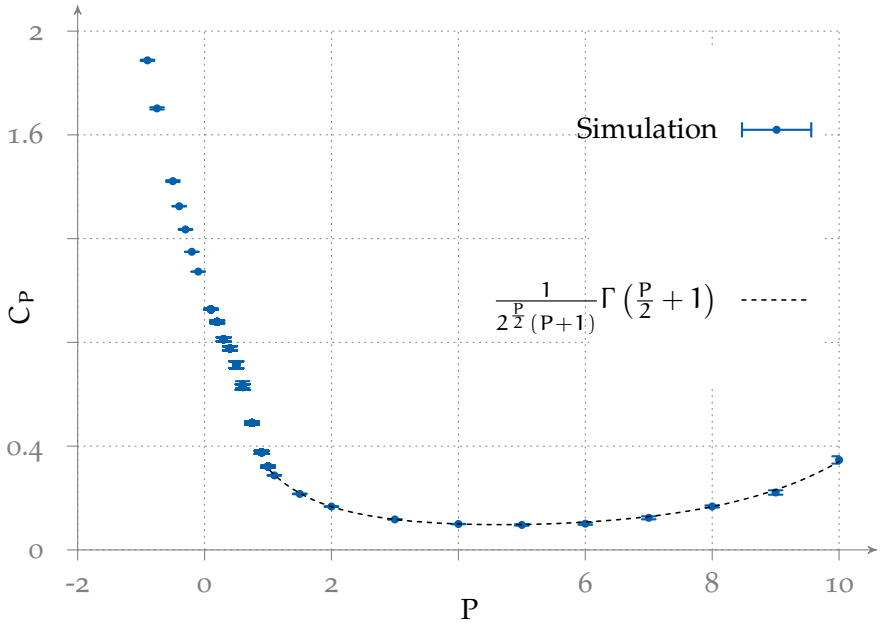

(a) Extrapolated free energy density C_P in the whole range of simulations.

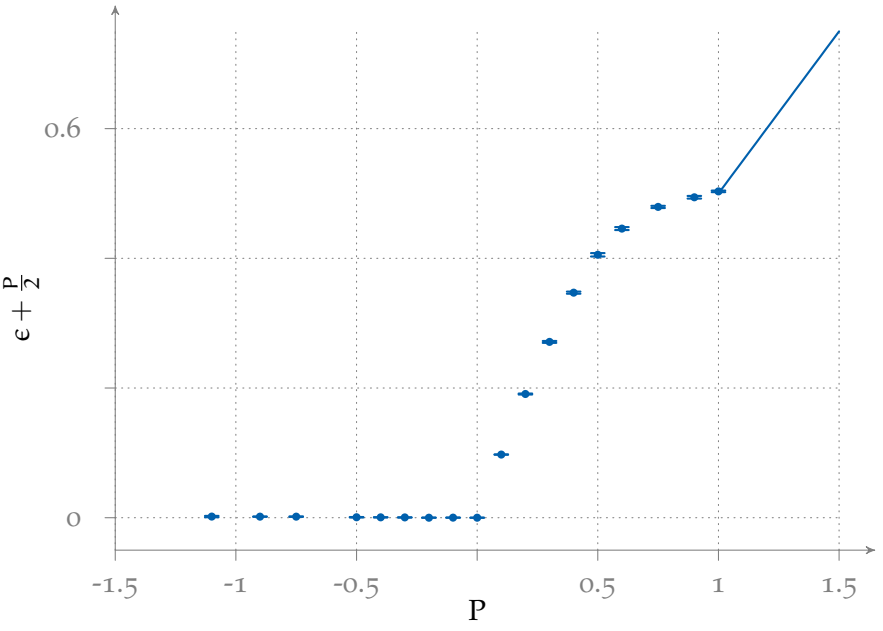

(b) Deviation from the scaling regime of the convex case.

Figure 18: Plot of the results presented in table 2.

3.4 EBMP IN GENERAL DIMENSION

The EBMP in $D > 1$ was also intensively studied, both in his scaling behavior and, more recently in its subleading corrections. This model showed some rich feature that it is worth discussing with a cronological point of view.

In Mézard and Parisi, 1988 was observed that once $2n$ points $-n$ of one type and n of the other– at fixed volume are given, the measure of the typical region in which a point of one type sees the nearest point of the other type is of the order $\sim \frac{1}{n}$, or, restated differently, that the typical distance between nearest neighbors in D dimensions scales as $\frac{1}{n^{1/D}}$. Hence one expects that (11) scales as $n^{1-\frac{p}{D}}$ in the thermodynamic limit.

In fact this argument was rigorously stated for $D \geqslant 3$ and *for every norm* in Talagrand, 1992. This argument is extensively used in the following.

Moreover it was proved in Ajtai et al., 1984 that in the bipartite case in $D = 2$ a logarithmic sub-leading correction comes out, the first correction to scaling behavior of a functional of the type (11) (apart for an unessential $\frac{1}{n}$) with costs defined in (18) being $O\left(\left(\frac{\log n}{n}\right)^{\frac{p}{2}}\right)$.

So a major point comes out: the sub-leading corrections in the monopartite and bipartite cases seems to differ. In fact in Houdayer et al., 1998 it is showed (and numerically confirmed) that the first correction to the scaling behavior is of the order $\frac{1}{n}$.

Whereas in the monopartite case, where all points are of the same type, the argument of proximity can be repeated at arbitrary small scales around a fixed position by increasing consistently n, in the bipartite case at low dimensions long range coupling of points may be necessary to realize the optimum frustrating the system.

The role of the local fluctuations of the density of points of the same type was at the heart of the ansatz proposed in Caracciolo, Lucibello, et al., 2014, in which it is predicted that the relevant exponent of the sub-leading correction is

$$\gamma_D = \frac{D-2}{D} \tag{43}$$

Since this result will play a crucial role in the following, this may be the place for a brief recall of the reasoning behind it, of course refering the interest reader to this paper for details.

The motivation for this ansatz comes from the continuous version of the euclidean bipartite matching problem, called the *Monge-Kantorovich problem*, for which a lot of rigorous results were proven (see for example Evans and Villani).

Consider for example two non negative measures with equal finite mass $\mu_+, \mu_- : \mathbb{T}^D \to \mathbb{R}^+$, where $\mathbb{T}^D$ is the standard D-torus obtained identifying opposite sides of the unit cube in D dimensions.

One can study the properties of certain measure preserving maps $\mathcal{M}^* : \mathbb{T}^D \to \mathbb{T}^D$, that is, a map such that $\forall f \in \mathcal{C}^1\left(\mathbb{T}^D\right)$,

$$\int_{\text{spt}\mu^+} f\left(\mathcal{M}(x)\right)\, d\mu^+(x) = \int_{\text{spt}\mu^-} f(x)\, d\mu^-(x) \tag{44}$$

which, if the measures have densities, is equivalent to the "change of variables" formula

$$\mu^+(s) = \mu^-\left(\mathcal{M}(s)\right) \det J_{\mathcal{M}}(s)\ \forall s \in \mathbb{T}^D \tag{45}$$

where $J_{\mathcal{M}}(s)_{ij} = \frac{\partial \mathcal{M}_i}{\partial s_j}$ is the Jacobian of the transformation. One then searches for minima of the *work* functional

$$W\left[\mathcal{M}; c\right] = \int_{\mathbb{T}^D} c(x, \mathcal{M})\, d\mu^+(x) \tag{46}$$

where $c : \mathbb{T}^D \times \mathbb{T}^D \to \mathbb{R}^+$ is a positive definite function called *the cost*.

When $c(x, y) = \|x - y\|^2$ it was proved in Evans, 1997 that the optimal map $\mathcal{M}^*$ admits a convex potential ϕ^*. Inserting this result in equation (45) and assuming $\mu^+(y) = \rho^+(y)dy$ and $\mu^-(y) = \rho^-(y)dy$ shows that ϕ^* satisfies the *Monge-Ampère equation*

$$\rho^+(y) = \det H_\phi(y)\rho^-\left(\nabla\phi(y)\right)$$

Observe now that, by supposing $\mathcal{M}^* = (\mathbb{1} + m(x))\, x$ (where $\|m(x)\| \ll 1$ throughout the torus) and that the densities satisfy $\rho^+ = 1 + \delta\rho^+$ and $\rho^- = 1 + \delta\rho^-$ with again $\delta\rho^+$, $\delta\rho^-$ small, equation (45) becomes

$$\Delta\psi = \delta\rho \tag{47}$$

which is the Poisson equation for the electrostatic potential ψ that generates (apart for a sign) the field $m(x) = \nabla\psi$, given the distribution of charges $\delta\rho = \rho^+ - \rho^-$.

So at first order the the cost is given by the kinetic energy term

$$W_2\left[\mathcal{M}\right] \sim \int_{\mathbb{T}^D} \nabla\psi(x) \cdot \nabla\psi(x)\, dx = \sum_{n \in \mathbb{Z}^D \setminus \{0\}} \frac{|\delta\hat{\rho}_n|^2}{4\pi^2 \|n\|^2} \tag{48}$$

where

$$\delta\hat{\rho}_n := \int_{\mathbb{T}^D} \delta\rho(x) e^{-2\pi i n \cdot x}\, dx$$

is the Fourier mode of $\delta\rho(x)$.

This analogy with electrostatics in the case of quadratic cost may be stressed also from another point of view. Considering the two empirical measures

$$\begin{aligned} \rho^+(x) &:= \frac{1}{n}\sum_{i=1}^{n} \delta^{(D)}(x - w_i) \\ \rho^-(x) &:= \frac{1}{n}\sum_{i=1}^{n} \delta^{(D)}(x - b_i) \end{aligned} \tag{49}$$

where $\{w_i\}_{i=1}^n$ and $\{b_i\}_{i=1}^n$ are i.i.r.v. on $\mathbb{T}^D$. Upon defining the "transport field" $\mu_{b_j}(w_i) := b_j - w_i$ one recovers the matching cost (18) if in the functional

$$E[\mu] = \int_{\mathbb{T}^D} \|\mu(y)\|^2 \rho^+(y)\, dy \tag{50}$$

the field is subject to the constraint

$$\int_{\mathbb{T}^D} \delta^{(D)}(x - y - \mu(y))\rho^+(y)\, dy = \rho^-(x)$$

which, roughly speaking, says that if one is located on a D-dimensional black point, one can reach a white point (bijectively) by a translation given by the transport field. In this way it is possible a formulation of the quadratic EBMP introducing a certain Lagrange multiplier ψ in the action

$$\begin{aligned} S[\mu,\psi] :=& \frac{1}{2}E[\mu] + \int_{\mathbb{T}^D} \psi(x)\left[\rho^-(x) - \int_{\mathbb{T}^D} \delta^{(D)}(x - y - \mu(y))\rho^+(y)\right] dx \\ =& \frac{1}{2}E[\mu] - \int_{\mathbb{T}^D} \psi(x)\rho(x) + \rho^+(x)\,(\mu(x)\cdot\nabla)\,\psi(x)\, dx + O\left(\|\mu\|^2\psi\right) \end{aligned} \tag{51}$$

where $\rho(x) := \rho^+(x) - \rho^-(x)$ is again the density of charge (see equation (47) for comparison).

So imposing stationarity to the functional (51), at first order in the norm of the transport field implies the coupled PDEs

$$\begin{cases} \rho(x) = \nabla\cdot(\eta(x)\mu(x)) \\ \mu(x) = \nabla\psi(x) \end{cases} \tag{52}$$

where $\eta(x)$ is the weak-limit $n \to \infty$ of both $\rho^+(x)$ and $\rho^-(x)$, that is, the distribution from which black and whites are extracted.

This is the classical electrostatic problem of finding the field $\mu(x)$ generated by a globally neutral configuration of charges (the respective distributions being the ones in (49)), in a medium with a stochastic permittivity $\eta(x)$. Note that the Lagrange multiplier ψ equals minus the electrostatic potential.

This observation unlocks tools from Green's function formalism, as widely discussed in Caracciolo and Sicuro, 2015a and Caracciolo and Sicuro, 2015b.

Consider the Fourier modes of $\delta\rho$: by recalling the decomposition (48) in the functional

$$\mathcal{E}_N[\delta\hat{\rho}] \equiv \sum_{n\in\mathbb{Z}^D\setminus\{0\}} \frac{|\delta\hat{\rho}_n|^2}{4\pi^2\|n\|^2} \tag{53}$$

captures the sub-leading corrections for the asymptotic behavior of (11) or in other words,in the case $P = 2$ upon defining

$$n^{\frac{2}{D}-1} C(\pi^*) = e_D^{(2)} + O\left(n^{-\gamma_D}\right) \equiv \beta_n^{(2)} \qquad D > 2$$

it must be true that

$$\beta_n^{(2)}(D) \sim n^{\frac{2}{D}} \sum_{n\in\mathbb{Z}^D\setminus\{0\}} \frac{\overline{|\delta\hat{\rho}_n|^2}}{4\pi^2\|n\|^2} = n^{-\gamma_D} \sum_{n\in\mathbb{Z}^D\setminus\{0\}} \frac{1}{2\pi^2\|n\|^2} \tag{54}$$

where in the last equality the mean over positions of the points on $\mathbb{T}^D$ –denoted as $\overline{\cdots}$– has been performed.

Formula (54), which is divergent in $D \geqslant 2$, was studied under a proper regularization scheme in Caracciolo, Lucibello, et al., 2014. This regularization gives the leading scaling behavior in $D = 2$ and both the leading and sub-leading corrections mentioned before in $D \geqslant 3$, as confirmed by their numerical results.

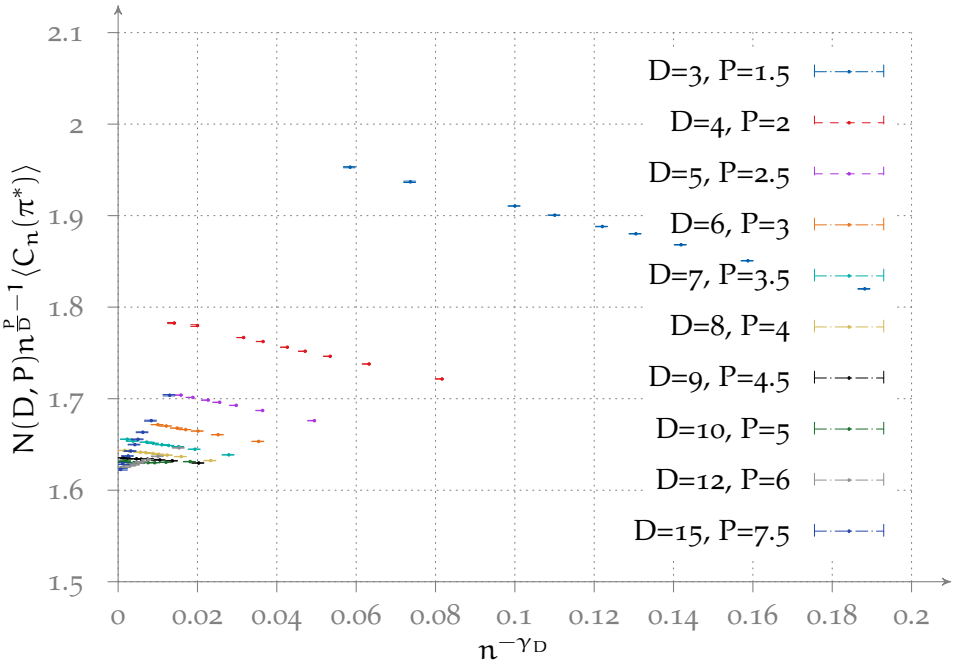

Figure 19: Typical output encountered during the numerical studies. This figure depicts the EBMP with PBC and shows the goodness of the ansatz discussed in 3.4 (the inessential constant $N(D,P)$ is defined in equation (58)).

3.4.1 Numerical results in $D \geqslant 3$

As mentioned in the previous section a rigorous foundation of the validity of ansatz (43) for arbitrary P has not yet been done. In the same spirit of the concluding remarks of Caracciolo, Lucibello, et al., 2014, it was chosen to simulate the EBMP in a Poisson-Poisson setting (i.e. blacks and whites are i.d.r.v. in $[0,1]^D$, with PBC imposed.

Numerical results were fitted with a three parameter function

$$n^{\frac{P}{D}-1}\langle C_n(\pi^*)\rangle = e_D^{(P)}\left(1+\frac{a_D^{(P)}}{n^{\gamma_D}}+\frac{b_D^{(P)}}{n^{2\gamma_D}}\right) \tag{55}$$

at least in the case with periodic boundary conditions there is strong numerical evidence that the γ_D ansatz holds for generic P.

Many comments are in order. In this case there is a strong numerical evidence for a change of sign of the quantity $a_D^{(P)}$ defined in (55)(or, possibly, of a restriction of the scaling region where ansatz (55) holds). A reasonable argument for a behavior of this kind is lacking, the only observation being that a limit optimal cost reached from above as

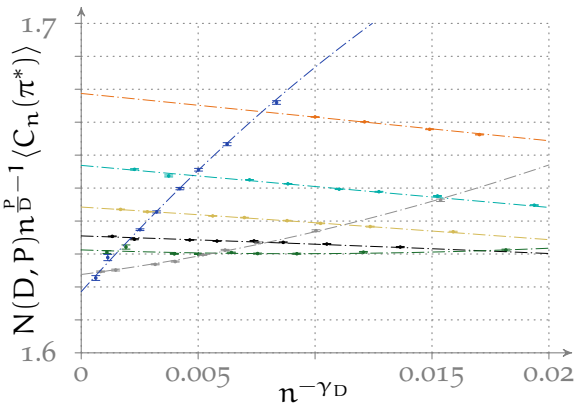

Figure 20: Zooming in figure 19.

shown in figure 20 opens the question on how corrections in the frustrated system reach their counterparts in the non-frustrated model, which, as strongly suggested numerically from 14, do have negative sign.

A more intriguing scenario with sub-leading corrections coefficients having positive signs, and not well fitted with the γ_D scaling ansatz emerged from the same problem with OBC. In this case the average optimal cost as a function of the size showed two distinct regimes:

1. A transient region showing a peak at some $n^* \leqslant 100$. At fixed dimension this maximum $n^*(P) < n^*(P')$ if $P < P'$.

2. An asymptotic region of very slow decrease towards the same limit value $e_D^{(P)}$ found by imposing periodic boundary conditions. Even if this feature appeared very clearly upon plotting results (an example of this plot is in figure 21), fitting data via (55) proved inadequate.

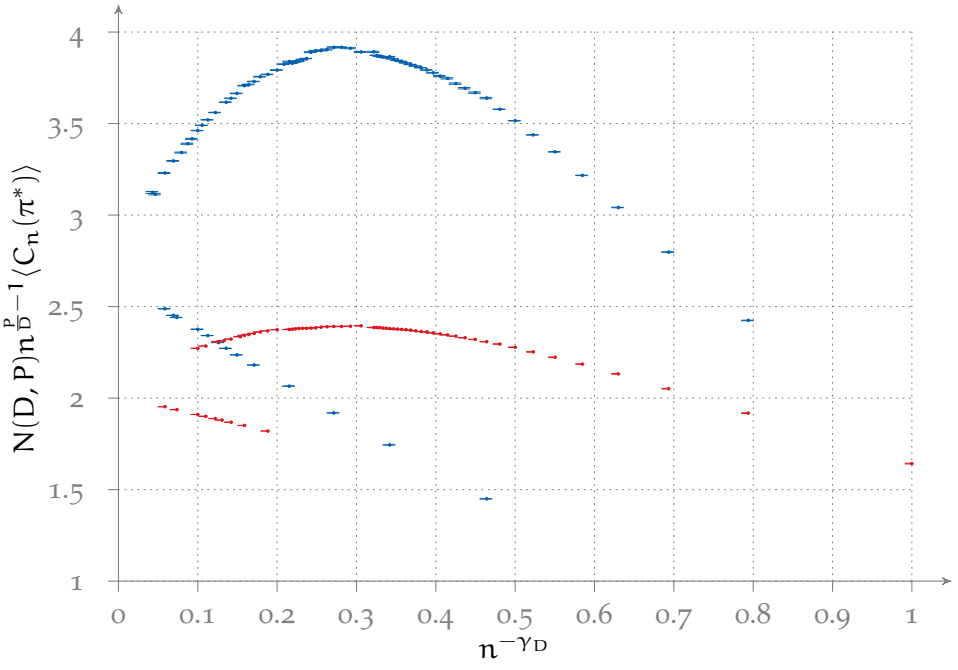

Figure 21: Comparison of the EBMP with P=D=3 (blue) and D=2P=3 (red). For each case, both results with open and periodic boundary conditions are depicted, the latter being respectively the blue and red concave curves.

3.5 RAP AS THE MEAN FIELD APPROXIMATION OF THE EBMP

3.5.1 General remarks

By noting that $\lim_{D\to\infty}\gamma_D = 1$ one can be interested in how the results discussed in section 3.2 are recovered. Moreover, at low dimensions –as expected from the arguments discussed in the previous section–, γ_D is fairly different from the exponent of the sub-leading correction in the Euclidean monopartite case (see Houdayer et al., 1998).

To properly compare the Euclidean bipartite matching problem, that has cost (18) and the random assignment problem it is necessary to normalize the distributions.

Observing that the probability density for a point in D dimensions to find a neighbor at a certain distance x is simply the measure of the D-sphere of radius x

$$\rho_D(x) = \frac{2\pi^{\frac{D}{2}}}{\Gamma\left(\frac{D}{2}\right)}x^{D-1} \equiv S_D(x) \tag{56}$$

In this way if $x \sim w^{\frac{1}{P}}$, it follows that

$$\rho_D(x)dx = \rho_D(w^{\frac{1}{P}})d\left(w^{\frac{1}{P}}\right) = S_D(1)\frac{w^{\frac{D}{P}-1}}{P}dw := \rho_{D,P}(w)dw \tag{57}$$

So by imposing equality on a small volume (subscripts R and E refers respectively to the Random and Euclidean case) it must be true that

$$\frac{w_R^r}{r!}dw_R = \rho_{D,P}(w_E)dw_E$$

What this relation implies is the existence of a proper "renormalizing" quantity depending only on D and P

$$N(D,P) := \frac{w_R}{w_E} = \left[\frac{S_D(1)\Gamma\left(\frac{D}{P}\right)}{P}\right]^{\frac{P}{D}} \tag{58}$$

under the constraint

$$r = \frac{D}{P} - 1 \tag{59}$$

These facts being cleared, to study how the mean field limit associated to the parameter r is reached it was proceeded as follows:

- For each accessible dimension D, it was simulated an Euclidean bipartite matching problem with cost (18), where

  $$P = r(D+1)$$

  .

  Periodic boundary conditions were chosen due to the simpler behavior observed in reaching a thermodynamic limit (as shown in 21).

- For every such problem, extrapolation in order to obtain the limit average optimal cost is done via (55); this value is then multiplied by (58). Thus, at fixed r, the typical output of a simulation is similar to the one plotted in figure (19) (which refers to the case $r = 1$).

3.5.2 Numerical investigation

An extensive numerical simulation of the EBMP with periodic boundary conditions was done in order to explore the connection to its mean field limit $D \to \infty$, with the caveats mentioned in the previous section.

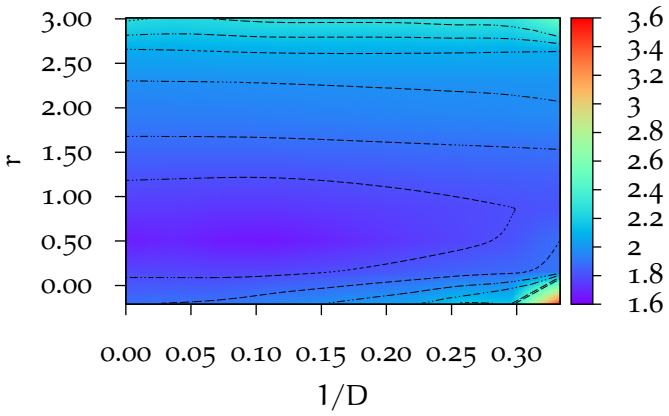

Figure 22: Density plot for the surface of renormalized costs in the EBMP on $\mathbb{T}^D$. Figure 13 is the section of this figure at $\frac{1}{D} = 0$.

Using the already mentioned fitting function (55) of section 3.5.1 it was decided to reconstruct the bi-dimensional landscape of the renormalized optimal cost, that is, to plot its value as a function of both r and D, with r and D constrained by (59).

At this point one can choose two approaches: the first is studying the renormalized optimal cost at fixed dimension D as a function of r, the expected qualitative trend being similar to the one in figure 13; the other is to study this landscape in the orthogonal direction, where one would expect sections at fixed r to have a qualitative decreasing monotone trend when D increases, the intuitive idea being that the optimal cost of a matching for the system constrained by euclidean geometry should be higher at lower dimension and should attain its minigm when frustration vanishes, i.e. in the completely random case. In fact this turned out to be true.

Since in $D = 2$ a logarithmic correction appears for the Euclidean bipartite matching problem (as discussed in Caracciolo, Lucibello, et al., 2014), S.Caracciolo proposed a relation of the type

$$w_r\left(\frac{1}{D}\right) = w_r\left(1 + u_r \frac{1}{D^2} \frac{1}{\left(1 - \frac{4}{D^2}\right)}\right) \tag{60}$$

the results of this fits are collected in table 4.

r \ D	3	4	5	6	7	8
-0.2	3.451(9)	2.5167(9)	2.220(2)	2.0827(5)	2.0159(8)	1.969(1)
-0.1	2.952(1)	2.402(4)	2.0071(9)	1.8984(8)	1.8420(5)	1.8053(4)
0	2.644(2)	2.0639(6)	1.8740(3)	1.7829(5)	1.7361(3)	1.7046(4)
0.25	2.240(2)	1.8502(6)	1.714(1)	1.6491(4)	1.610(2)	1.5920(7)
0.5	2.086(5)	1.776(8)	1.6177(4)	1.5895(3)	1.5713(9)	1.5595(2)
0.75	2.0206(4)	1.7670(7)	1.6789(2)	1.6345(2)	1.6117(4)	1.5951(7)
1	2.0117(6)	1.796(1)	1.7170(2)	1.6787(2)	1.6569(5)	1.6442(1)
2	2.1910(7)	2.0400(1)	1.9867(1)	1.95987(9)	1.9438(2)	1.9347(1)
3	2.4880(5)	2.3698(1)	2.32441(4)	2.3007(1)	2.2897(1)	2.2816(2)

r \ D	9	10	12	15	∞
-0.2	1.943(2)	1.925(2)	1.897(6)	1.889(4)	1.8846(3)
-0.1	1.7842(6)	1.764(1)	1.7490(2)	1.751(4)	1.7357(3)
0	1.6864(3)	1.6725(3)	1.6565(9)	1.6478(6)	$\frac{\pi^2}{6}$
0.25	1.5768(3)	1.5685(7)	1.554(1)	1.550(3)	1.5458(1)
0.5	1.5595(2)	1.5530(4)	1.5412(3)	1.5377(3)	1.53525(8)
0.75	1.5876(2)	1.5805(5)	1.5710(8)	1.568(1)	1.5654(1)
1	1.6355(4)	1.6312(8)	1.6238(8)	1.619(1)	1.61698(8)
2	1.9283(2)	1.9243(2)	1.9186(2)	1.9176(9)	1.91456(7)
3	2.2757(3)	2.2726(1)	2.2680(4)	2.2667(9)	2.26430(9)

Table 3: The numerics obtained in the study of the $D \to \infty$ limit. Each entry of the table (except the ones corresponding to $D = \infty$) is obtained via extrapolation with (55). The e_D^P obtained in this way (see (55) for its definition) is re-scaled by the relevant $N(D, P)$ defined in eq. (58).

Table 4: Results of interpolation with function (60). Each row defines a function; all 9 functions are plotted in figure 23.

r	w_r	u_r
-0.2	1.876(6)	3.8(1)
-0.1	1.718(6)	3.57(8)
0	1.640(3)	2.91(1)
0.25	1.544(2)	2.26(6)
0.5	1.524(2)	1.91(3)
0.75	1.564(1)	1.47(2)
1	1.611(1)	1.29(3)
2	1.913(1)	0.79(1)
3	2.263(1)	0.55(1)

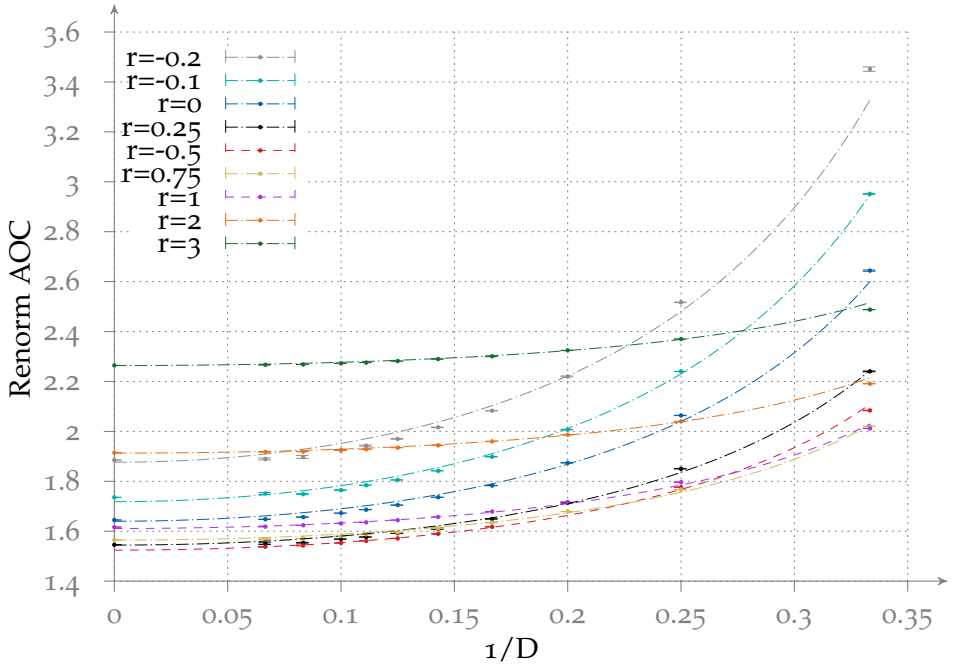

Figure 23: Slices at fixed r of figure 22 show that mean field predictions may differ sensibly from Euclidean average optimal cost when $r \leqslant 0$, while in the $r = 3$ class the greatest deviation from mean field AOC is 7%, achieved in $D = 3$.

3.6 CONCLUSIONS AND FUTURE WORK

Both the random assignment problem and the Euclidean bipartite matching problem have been studied by means of the Jonker-Volgenant algorithm that solves the general linear sum assignment problem in $O(n^3)$ time.

Results matched very well both theoretical predictions –where available– and are consistent with numerical data previously known in the literature.

It is possible to summarize them as follows:

- In the random assignment problem, there is strong numerical evidence of a peaking property for the re-scaled averaged optimal cost throughout the whole region $r \in [-1, 3]$. The distribution of these quantities proved to be very well fitted by gaussians distributions, but of course this is not sufficient to prove that they are self-averaging. It was possible to extract coefficients of the $\frac{1}{N}$ corrections, as showed in figure 14. Extrapolations of coefficients for the $\frac{1}{N^2}$ corrections are less precise and require a deeper numerical analysis.

- In the one dimensional grid-Poisson Euclidean bipartite matching problem with open boundary conditions with cost (18) when $P > 1$, simulations agrees to their last digit precision with analytic predictions for the averaged optimal cost in the thermodynamic limit computed as explained in Caracciolo, Sergio and Sicuro, Gabriele, 2014; moreover, in the region $P \in [-1.1, 1]$ where the previous approach is not possible, and where to the best of author's knowledge no prediction for the AOC value has yet been done, there is strong numerical evidence of a deviation from convex scaling, these data being summarized in table 2.

- In the EBMP in $D > 3$ for general P, in the case with PBC, numerical findings are in excellent agreement with the numerical data found in Caracciolo, Lucibello, et al., 2014, strongly supporting their scaling ansatz for the sub-leading correction; the coefficients of these corrections showed an intriguing feature, being negative at sufficiently low dimensions, and changing sign around $D \sim 10$.

- In the EBMP in $D > 3$ for general P, in the case with OBC, again numerical findings for the limit value of the average optimal cost match very well their counterparts in the case with PBC. However in this case there is numerical evidence that signs of the $\frac{1}{N}$ corrections stay positive throughout all the dimensions numerically investigated.

- The relationship between the random assignment problem and the Euclidean bipartite matching problem with PBC was numerically studied. An entire bi-dimensional landscape was created, this construction allowing a $\frac{1}{D}$ expansion for a renormalized Euclidean AOC with respect to the Random assignment, this value being reached when $D \to \infty$.

A first and general step to be implemented in order to deepen the study of these disordered and frustrated systems may come from studying correlation functions. Studying these quantities from the point of view of critical exponent theory can shine light on how the quantities discussed in this work reach the thermodynamic limit together with their sub-leading corrections.

It may be very interesting a numerical study of the distribution of the costs in the optimal matching as a function of n. Accessing the distribution of link's weight in the optimal configuration –it may be called an occupancy distribution– can shine light on the properties of the ground states of such models and how their fluctuations behave when $n \to \infty$; already in the $r = 0$ class for the random assignment problem, as shown in Mézard and Parisi, 1985, these distributions can be far from trivial.

Moreover one can study how the sub-leading corrections coefficients of the Euclidean bipartite matching problem reach the random assignment corrections in the $D \to \infty$ mean field limit: as shown in figure 20, it is not clear how this can happen and why a change of sign should happen. This phenomenon is more evident in the EBMP with open boundary conditions.

A possible way to implement the featured mentioned is by means of a careful rethinking of the optimisation procedure, which now can only output the optimal cost but; a program for studying correlation functions must be able to output the optimal matching at fixed disorder for every instance without penalizing (too much) performances.

Another plausible direction of future work is to extensively study a general assignment problem weakening assumptions on the cost function, such as densities with unbounded support, such as the region $r < -1$, where power law distributions of the type 13 come outside the gaussian universality class.

Code updating is already in progress.

A APPENDIX

A.1 GRAPH THEORY

A.1.1 Simple spectral properties of K_n

The computation of the characteristic polynomial of $Ad(K_n)$ consists in the determination of $\det(\lambda \mathbf{1}_n - Ad(K_n))$, where $Ad(K_n)$ is the matrix in equation 2. This can be accomplished by observing that $Ad(K_n)_{ij} = 1 - \delta_{ij}$ by a root-by-root summation (due to compatibility of the operators). The result is

$$P_n(\lambda) = (-)^n(\lambda+1)^{(n-1)}(\lambda-(n-1)) \tag{61}$$

from which follows the recurrence relation

$$P'_n = -nP_{n-1}$$

One way of summarizing all this is by means of the exponential bi-dimensional generating function $\Gamma(\lambda, t)$ obtained by multiplying the two sides of eq. (A.1.1) by $\frac{t^n}{n!}$ and then summing over n, the n-th characteristic polynomial being $P_n(\lambda) = \frac{\partial^n}{\partial t^n}\Gamma(\lambda, t)|_{t=0}$.

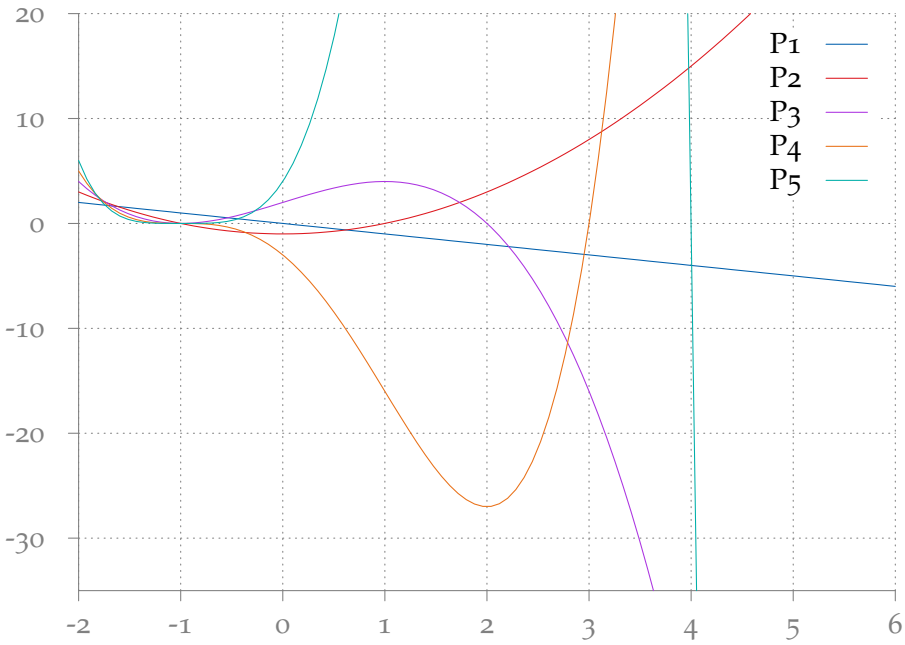

Figure 24: P_n as defined in eq (61) for $n = 1, \ldots, 5$ has nondegenerate integer roots at $n-1$.

Recalling that $P_1 = -\lambda$ takes to the Cauchy problem

$$\begin{cases} \frac{\partial \Gamma}{\partial \lambda} = -t\Gamma \\ \frac{\partial \Gamma}{\partial t}|_{t=0} = -\lambda \end{cases}$$

whose solution is $\Gamma(t, \lambda) = (1+t)e^{-t(\lambda+1)}$.

A.1.2 Hall's or Marriage theorem

Theorem 4 (P.Hall 1935)**.** *In a bipartite graph $G_{U,V}$ where $s = |U| \leqslant |V|$ there exists a matching M such that $|M| = s$ if and only if G satisfies Hall's condition.*

Actually this theorem was proved in a different contest. A family of sets $\{S_i\}_{i=1}^n$, admits a *system of distinct representatives* if n distinct elements e_i, $i = 1, \ldots, n$ can be chosen in such a way that $e_i \in S_i$ $i = 1, \ldots, n$; in this setting the theorem states that *the family $\{S_i\}_{i=1}^n$ admits a complete system of distinct representatives if and only if $\forall m$ any union of m S_i's has at least cardinality m.*

In Hall, 1935 the author also deduces as a corollary the graph theoretic analogue of this theorem, the one of interest in this work, proved by Konig almost 20 years earlier in König, 1916.

Proof. Necessity. If the condition fails there exists at least one $W \subseteq U$ with too few neighbors (i.e. $|N(W)| < W$). Then W cannot be matched to any $X \subset V$ and even more so U.

Sufficiency. Constructively by induction on s: the statement is clearly true for $s = 1$; supposing the statement true at step s, that is, if in a bipartite graph $G_{U,V}$ every $U_1 \subset U$, $|U| = s+1$ with size at most s satisfies Hall's condition, then the *entire* U can be matched to V (step $s+1$). There could be two cases.

EVERY $A \subset U$ SATISFIES HALL'S CONDITION STRICTLY, $|N(A)| > |A|$

By hypothesis a vertex $u \in U$ is such that $|N(U)| \geqslant 2$, so that we can match it to one of its neighbors $v \in V$; consider now the bipartite graph $G'_{U\setminus\{u\},V\setminus\{v\}}$ induced by the removal of the edge uv. The set $U' = U \setminus \{u\}$ then satisfies Hall's condition, which by induction hypothesis, implies that it can be matched to $V' = V \setminus \{v\}$ by a matching M' of cardinality s. We have provided a matching $M = M' \cup uv$, $|M| = s+1$ for the entire $G_{U,V}$.

THERE EXISTS $A \subset U$ FOR WHICH $|N(A)| = |A|$

By induction hypothesis A can be matched by a matching M' to a subset of $N(A)$, in fact the whole $N(A)$ (since the two sets have the same cardinality). Again consider the bipartite graph $G''_{U'',V''}$, where $U'' = U \setminus A$ and $V'' = V \setminus N(A)$. Then an arbitrary $B \subseteq U''$ satisfies Hall's condition with its neighborhood

in G'', namely $|N(B) \cap V''| \geqslant |B|$. Since $B \cap A = \emptyset$ (and since for hypothesis $A \cup B$ satisfies Hall's condition) follows that

$$|N(A)| + |N(B) \cap V''| = |N(A \cup B)| \geqslant |A \cup B| = |A| + |B|$$

So G'' has a matching M'' and $M' \cup M''$ is a matching for the whole G.

□

A.1.3 The Birkhoff-von Neumann theorem

Theorem 5. *Every doubly stochastic matrix is a convex combination of* $n \times n$ *permutation matrices.*

Proof. By simple algebraic properties of the matrix addition it is clear that a convex combination of doubly stochastic matrices is doubly stochastic. So the assignment polytope is closed under convex combinations. To prove the theorem is then sufficient to show that every permutation matrices is the vertices of Birkhoff's polytope. For this purpose observe that every doubly stochastic matrix w is the weighted adjacency matrix of a bipartite graph $G_{U,V}$, where U is associated to rows and V to columns. This graph is in general a subgraph of $K_{n,n}$ and, since any row or column of a doubly stochastic matrix sums to 1, the total weighted degree entering any vertices (the sum of weights on links connecting a vertex $u \in U$ to any neighbor $v \in N(u) \subseteq V$ is one. It is clear that $G_{U,V}$ and satisfies Hall's condition. Indeed, given $S \subseteq U$

$$\begin{aligned} |N(S)| = \sum_{\substack{v_i \in N(S) \subseteq V \\ u_j \in N(N(S)) \subseteq U}} w_{ij} \geqslant \sum_{\substack{v_i \in N(S) \subseteq V \\ u_j \in S \subseteq U}} w_{ij} = \sum_{u_i \in S} 1 \\ = |S| \end{aligned} \tag{62}$$

By theorem 4 $G_{U,V}$ has a perfect matching, say M_1. By choosing the minimum weight λ_0 entering the matching M_1 consider the matrix

$$\overline{M}_1 = \lambda_0 P_1 \tag{63}$$

where P_1 is the permutation matrix associated to matching M_1. It follows that matrix

$$w' = \frac{1}{1 - \lambda_0} w - \overline{M}_1 \tag{64}$$

is again a doubly stochastic matrix, associated to a bipartite graph $G'_{U,V}$ where the minimum weight link figuring in perfect matching has been removed. This procedure can be repeated at most n^2 (the number of links in a bipartite graph $K_{n,n}$), showing constructively that it is possible to express every doubly stochastic matrix as a convex combination of permutation matrices P_i with coefficients λ_i. □

A.2 RAP AND EUCLIDEAN BIPARTITE MATCHING PROBLEM

A.2.1 The Brownian bridge

A *Brownian bridge* is the continuous stochastic process defined by

$$B(t) := W(t) - tW(1) \qquad t \in [0,1]$$

where $W(t)$ is the standard Brownian motion on $[0,1]$. It is a centered process with covariance

$$\begin{aligned}\mathbb{E}(B(t')B(t)) =& \mathbb{E}\left[\left(W(t)+W(t')-W(t)\right)W(t)\right] - tt' \\ =& \mathbb{E}(W^2(t)) + \mathbb{E}\left[\left(W(t')-W(t)\right)W(t)\right] - tt' \\ =& t(1-t') \quad \text{if } t \leqslant t' \\ =& t'(1-t) \quad \text{if } t' \leqslant t\end{aligned}$$

since $W(\tau)$ is a normal random variable with variance τ whose increments are independent. A modern reference for the theory of continuous time stochastic processes and in particular Brownian motion is Karatzas and Shreve, 1998.

The realizations of this process are maximally spread at $t = \frac{1}{2}$, the motion being more and more deterministic approaching the $t = 0, 1$.

A way to see how this conditioning happens is by mean of the conditional probability to go at height y at time s, coming from height x at time t ($s > t$):

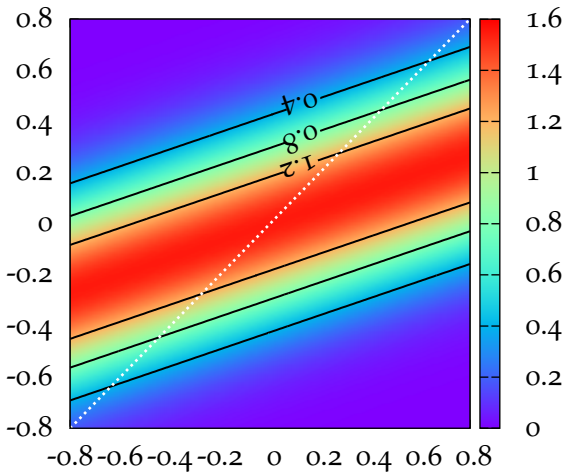

Figure 25: Conditional probability density for a Brownian bridge to be at height y at time t=0.9 if it was at height x at time t=0.7. Note that the density peaks under the bisector (the dashed white line), telling that the more the path departs from the x(t)=0 axis, the higher is the probability of reverting back.

$$\begin{aligned}p(B(s)=y|B(t)=x) =& \\ \frac{p(B(t)=y, B(s)=x)}{p(B(s)=x)} =& \frac{\mathbb{E}\left[\delta(B(t)-y)\delta(B(s)-x)\right]}{\mathbb{E}\left[\delta(B(s)=x)\right]} = \\ =& \sqrt{\frac{1-t}{2\pi(s-t)(1-t)}}\, e^{-\frac{y^2}{2(1-s)} - \frac{(x-y)^2}{2(s-t)} + \frac{x^2}{2(1-t)}}\end{aligned} \tag{65}$$

B BIBLIOGRAPHY

Ajtai, M., J. Komlos, and G. Tusnady

1984 "On optimal matchings", *Combinatorica*, 2, 4, p. 259. (Cited on p. 41.)

Alexanderson, Gerald L.

2006 "About the cover: Euler and Koenigsberg's briges: a historical view", *Bull. Am. Math. Soc.*, 43, 4, pp. 567-573, DOI: 0273-0979(06)01130. (Cited on p. 5.)

Arnol'd, V.I.

2004 *Arnold's Problems*, Springer, Leipzig, ISBN: 3540207481. (Cited on p. 1.)

Boniolo, Elena, Caracciolo, Sergio, and Sportiello, Andrea

2014 "Correlation function for the Grid-Poisson Euclidean matching on a line and on a circle", arXiv: arXiv:1403.1836v3. (Cited on pp. 34, 36, 39.)

Brunetti, R, W. Krauth, Marc Mézard, and Giorgio Parisi

1991 "Extensive Numerical Simulations of Weighted Matchings : Total Length and Distribution of Links in the Optimal Solution ." *Europhysics Letters*, 14, 4, pp. 295-301. (Cited on p. 30.)

Burkard, Rainer E and Eranda Çela

1999 "Linear Assignment Problems and Extensions *". (Cited on pp. 17, 21.)

Caracciolo, Sergio and Sicuro, Gabriele

2014 "One-dimensional Euclidean matching problem: exact solutions, correlation functions, and universality." *Physical review. E, Statistical, nonlinear, and soft matter physics*, 90, 4 (Oct. 2014), p. 042112, ISSN: 1550-2376, DOI: 10.1103/PhysRevE.90.042112. (Cited on pp. 34, 36, 52.)

Caracciolo, Sergio, Carlo Lucibello, Giorgio Parisi, and Gabriele Sicuro

2014 "Scaling hypothesis for the Euclidean bipartite matching problem." *Physical review. E, Statistical, nonlinear, and soft matter physics*, 90, 1 (July 2014), p. 012118, DOI: 10.1103/PhysRevE.90.012118, arXiv: 1402.6993. (Cited on pp. 41, 44, 45, 49, 52.)

Caracciolo, Sergio and Gabriele Sicuro

2015a "Quadratic Stochastic Euclidean Bipartite Matching Problem." *Physical review letters*, 115, 23 (Dec. 2015), p. 230601, ISSN: 1079-7114, DOI: 10.1103/PhysRevLett.115.230601. (Cited on p. 43.)

2015b "Scaling hypothesis for the Euclidean bipartite matching problem. II. Correlation functions." *Physical review. E, Statistical, nonlinear, and soft matter physics*, 91, 6 (June 2015), p. 062125, ISSN: 1550-2376, DOI: 10.1103/PhysRevE.91.062125. (Cited on p. 43.)

Cerf, Nicolas J., Jacques H. Boutet de Monvel, Oriol Bohigas, Olivier C. Martin, and Allon G. Percus

1997 "The random link approximation for the Euclidean traveling salesman problem", *Journal de Physique I*, 7, January, pp. 117-136.

Chartrand, Gary and Ping Zhang

2012 *A first course in graph theory*, Dover Publications, Inc., p. 450. (Cited on pp. 5, 13.)

Dijkstra, E W

1956 "A Note on Two Problems in Connexion with Graphs", *Numer. Math.*, 1, pp. 269-271. (Cited on p. 12.)

Euler, Leonhard

1741 "Solutio Problematis ad Geometriam Situs Pertinentis", *Commentarii Academiae Scientiarum Imperialis Petropolitanae*, 8, pp. 128-140. (Cited on p. 5.)

Evans, Lawrence C.

1997 "Partial differential equations and Monge-Kantorovich mass transfer", *Curr. Dev. Math.*, http://math.berkeley.edu/%7B~%7Devans/Monge-Kantorovich.survey.pdf. (Cited on p. 42.)

Godsil, Chris and Gordon Royle

2001 *Algebraic Graph Theory*, ed. by S Axler, F W Gehring, and K A Ribet, Springer, p. 453. (Cited on p. 11.)

Hall, Philip

1935 "On Representatives of Subsets", *J. London Math. Soc.*, 10, 1, pp. 26-30, DOI: 10.1112/jlms/s1-10.37.26. (Cited on p. 56.)

Houdayer, Jérôme, J.H. Boutet de Monvel, and O.C. Martin

1998 "Comparing mean field and Euclidean matching problems", *Eur. Phys. J. B*, 6, 3 (Nov. 1998), pp. 383-393, ISSN: 1434-6028, DOI: 10.1007/s100510050565, arXiv: 9803195 [cond-mat]. (Cited on pp. 27, 30, 32, 41, 47.)

Jonker, R. and A. Volgenant

1987 "A shortest augmenting path algorithm for dense and sparse linear assignment problems", *Computing*, 38, 4, pp. 325-340, DOI: 10.1007/BF02278710. (Cited on pp. vi, 3, 17, 18.)

Karatzas, Ioannis and Steven E. Shreve

1998 *Brownian Motion and Stochastic Calculus*, ed. by S Axler, F W Gehring, and K A Ribet, Springer, p. 459. (Cited on p. 58.)

Kasteleyn, Pieter Willem

1961 "The statistics of dimers on a lattice: I. The number of dimer arrangements on a quadratic lattice", *Physica*, 27, 12 (Dec. 1961), pp. 1209-1225. (Cited on p. 2.)

König, Dénes

1916 "Über Graphen und ihre Anwendung auf Determinantentheorie und Mengenlehre", *Math. Ann.*, 77, 4 (Dec. 1916), pp. 453-465, DOI: 10.1007/BF01456961. (Cited on p. 56.)

1936 *Theorie der endlichen und unendlichen Graphen*, Akademische Verlagsgesellschaft, Leipzig, ISBN: 0817633898. (Cited on p. 5.)

Kruskal, Joseph B

1956 "On the shortest spanning subtree of a graph and the traveling salesman problem", *Proc. Amer. Math. Soc.*, 7, pp. 48-50. (Cited on p. 12.)

Kuhn, H. W.

1955 "The Hungarian method for the assignment and transportation problems", *Naval Research Logistics Quarterly*, 2, pp. 83-97. (Cited on pp. 17, 21.)

Lee, Yusin and James B Orlin

1993 "On Very Large Scale Assignment Problems", in *Large Scale Optimization: State of the Art*. (Cited on pp. 30, 32.)

McCann, Robert

1999 "Exact solutions to the transportation problem on the line", *Proc.R.Soc.A Math.,Phys. Eng Sci*, 455, pp. 1341-1380. (Cited on pp. 34, 36, 37.)

Mézard, Marc and Giorgio Parisi

1985 "Replicas and optimization", *Journal de Physique Lettres*, 46, 17, pp. 771-778, ISSN: 0302-072X, DOI: 10.1051/jphyslet:019850046017077100. (Cited on pp. vi, vii, 26, 29, 53.)

Mézard, Marc and Giorgio Parisi

1986a "A replica analysis of the travelling salesman problem", *Journal de Physique*, 47, 1986, pp. 1285-1296.

1986b "Mean-field equations for the matching and the travelling salesman problems", *Europhysics Letters*, 2, 12, pp. 913-918.

1987 "On the solution of the random link matching problems", *Journal de Physique*, 48, 9, pp. 1451-1459, ISSN: 0302-0738, DOI: 10.1051/jphys:019870048090145100.

1988 "The euclidean matching problem", *Journal de Physique*, 49, pp. 2019-2025. (Cited on pp. 31, 41.)

Parisi, Giorgio

1998 "A Conjecture on random bipartite matching", *ArXiV*, arXiv: 9801176 [cond-mat]. (Cited on p. 29.)

Sicuro, Gabriele

2014 *The Euclidean Matching Problem Statistical Physics Methods for Optimisation*, PhD thesis, Università di Pisa.

Steen, Maarten Van

2010 *Graph Theory and Complex Networks: An Introduction*, p. 300, ISBN: 9081540610. (Cited on p. 5.)

Talagrand, Michel

1992 "Matching random samples in many dimensions", *The Annals of Applied Probability*, 2, 4, pp. 846-856. (Cited on p. 41.)

Tutte, William Thomas

1984 *Graph Theory*, ed. by Gian-Carlo Rota, Addison-Wesley Publishing Company, p. 334. (Cited on pp. 5, 8.)